Nanocrystals & loaded porous silica for increased oral bioavailability

Inaugural-Dissertation

to obtain the academic degree

Doctor rerum naturalium (Dr. rer. nat.)

submitted to the Department of Biology, Chemistry and Pharmacy

of Freie Universität Berlin

by

Qionghua Wei

from Shaanxi, China

2016

The enclosed doctoral research work was performed under the supervision of Prof. Dr. Rainer H. Müller from February 2012 till August 2016 in the Institute of Pharmacy, Department of Pharmaceutical Technology, Biopharmaceutics & NutriCosmetics, Freie Universität Berlin.

1st Reviewer: Prof. Dr. Rainer H. Müller

2nd Reviewer: Prof. Dr. Matthias F. Melzig

Date of defense: May 9, 2017

To my parents, my husband and my dear daughters

With all my love and gratitude

Table of contents

1 Introduction and aims

1.1 Poorly soluble drugs for oral administration

Oral dosage form is considered as the most convenient and commonly employed route of drug delivery due to the ease of administration, high patient compliance, cost-effectiveness, least constraints and flexibility in the design (Krishnaiah 2010). Drug companies have invested extensive effort on the development of oral drug products. However, although several factors can affect the bioavailability of an orally administrated dosage, e.g. first-pass metabolism, pre-systemic metabolism and susceptibility to efflux mechanisms, poor aqueous solubility and low permeability have been proven as the most frequent causes of low bioavailability (Sakaeda, Okamura et al. 2001; Vieth, Siegel et al. 2004).

Based on drug aqueous solubility and intestinal permeability, a Biopharmaceutical Classification System (BCS) has been established to classify drug substances. Drugs are divided into four classes in BCS: Class 1, high solubility and high permeability, Class 2, low solubility but high permeability, Class 3, high solubility but low permeability, Class 4 low solubility and low permeability. The US Food and Drug Administration (FDA) defined that a substance is highly soluble when the highest dose in an immediate release oral product is soluble in 250 ml or less of aqueous media over the pH range of 1.0-7.5, otherwise, the compound is classified as poorly soluble; when the intestinal absorption of a drug substance is determined to be more than 90% based on mass balance or comparing to an intravenous reference dose it is considered highly permeable (Yu, Amidon et al. 2002).

Because of the introduction of combinational chemistry and high throughput screening, numerous drugs have been discovered as the new chemical entities with high molecular weight and lipophilicity, showing increasing poorly water-soluble characteristic. It is reported that 60% of the new chemical entities have a solubility below 100 μg/ml (Merisko-Liversidge, Liversidge et al. 2003). Moreover, in the commercialized drugs, about 40% of them have solubility lower than 100 μg/ml although with immediate release profiles (Takagi, Ramachandran et al. 2006). In the 100 products launched

between 1995 and 2002, more than half of drugs were categorized in Class 2 or Class 4 (Stegemann, Leveiller et al. 2007).

Saturation solubility is the value measured when the dissolved solute is in equilibrium with the undissolved solute. Poor solubility means low saturation solubility. Many problems are due to the poor saturation solubility of drug substances. For oral dosage form, low bioavailability is the major challenge. Aqueous saturation solubility is not only a determinant of its dissolution rate from solid dosage but also a prerequisite to drug absorption from the gastrointestinal tract. This is to say that the limited dissolution rate due to low aqueous saturation solubility causes the low bioavailability of orally administered drugs (Horter and Dressman 2001).

According to the Noyes-Whitney equation, low saturation solubility causes a decreased concentration gradient, which leads to a low dissolution rate.

$$\frac{dX}{dt} = \frac{DA}{h_D}\,(C_s - C_t) \qquad [1]$$

where dX/dt is the dissolution rate, D is the diffusion coefficient, A is the surface area, h_D is the diffusional distance, C_s is the saturation solubility, C_t is the concentration around the particles in the bulk phase.

Poor saturation solubility also correlates to the permeation and absorption of drug substances by passive diffusion. Drug flux (F) across an absorptive membrane can be described by the following equation, in which situation appropriate chemical and metabolic stability and an absence of transporter or carrier-mediated processes are assumed (Williams, Trevaskis et al. 2013; Prakash Khadka and Ro 2014):

$$F = \frac{D \cdot K \cdot A}{h}\,(C_m - C_0) \qquad [2]$$

where D is the diffusion coefficient of drug in the membrane, K is the partition coefficient between the aqueous solution overlaying the membrane and the membrane itself, A is the surface area, h is the width of the diffusion layer, C_m is the drug concentration adjacent to the membrane, C_0 is the drug concentration on the inner side of the membrane.

This equation shows that low drug concentration adjacent to the membrane due to poor saturation solubility leads to a decreased concentration gradient between gut lumen and blood, therefore a decreased drug absorption through the membrane.

Recognizing that drug solubility and permeability are the basic factors controlling the rate and extent of drug absorption, *in-vitro* drug dissolution and *in vivo* bioavailability are correlated based on the BCS (Amidon, Lennernas et al. 1995). Class 2 drugs, with low solubility and high permeability, can be ideal candidates for high bioavailability if the aqueous solubility is enhanced. Similarly, the technologies used for Class 2 drugs to improve the aqueous solubility together with absorption enhancer can be performed on Class 4 drugs (Kawabata, Wada et al. 2011).

Poor bioavailability not only causes problems during formulation development and clinical testing, but also leads to environment pollution through human waste. Drugs with low bioavailability are not completely absorbed and metabolized by patients. Drug residual is excreted into the sewage system, and when it is not processed properlyby sewage treatment plants it pollutes the environment (Kummerer 2001). Traces of pharmaceutical drugs have been detected in rivers and lakes (Ternes 1998). The detected compounds include hormones, pain killers, lipid regulators, antibiotics, anti-cancer drugs and blood pressure regulating drugs (Jones, Voulvoulis et al. 2001).

Finding ways to increase the drug solubility in aqueous solvent can improve bioavailability for more effective treatment of patients and be beneficial to the environment.

1.2 Nanocrystal to increase oral bioavailability

Particle size reduction is a traditional and effective approach to improve solubility of poorly water-soluble drugs because solubility is intrinsically related to drug particle size as long as the size is below approx. 1 μm. Micronization as the first size reduction method can work on any drug independent of its structure, however, it is non-effective for new developed drugs that possess significantly lower saturation solubilities

(Shegokar and Müller 2010). Micronization increases the dissolution velocity but not the saturation solubility. Instead of micronization, nanonization was introduced as an effective process to increase the saturation solubility of poorly water-soluble drugs (Brough and Williams 2013).

Drug nanocrystals are crystals with a size in the nanometer range, indicating they are nanoparticles with a crystalline character. The size range is considered different depending on the discipline. In colloid chemistry nanoparticles are defined as particles below 100 nm or even below 20 nm. However, in the pharmaceutical field nanoparticles with a size between a few nanometers and 1000 nm are all considered as nanoparticles. One obvious characteristic is that no carrier material is employed during the production of drug nanocrystals, thus the drug content in the product can be increased. Dispersed nanoparticles can be stabilized by surfactants or polymeric stabilizers in nanosuspensions, and the dispersion media can be water, aqueous solutions or non-aqueous solution (Müller and Akkar 2004).

Drug nanocrystals can overcome a series of solubility problems due to their special features, including an increase in saturation solubility, an improvement in dissolution rate, and an improved adhesiveness to surface/cell membrane (Müller, Gohla et al. 2011).

Thermodynamic saturation solubility is a compound-specific constant derived from physiochemical properties of the compound, dissolution medium and temperature. For nanocrystals, the saturation solubility (= kinetic saturation solubility) is also related to particle size. This phenomenon can be explained through the Kelvin and the Ostwald-Freundlich equations (Merisko-Liversidge, Liversidge et al. 2003; Moschwitzer and Müller 2006; Keck and Müller 2010).

The Kelvin equation describes how the vapor pressure of droplets increases due to curved liquid/vapor interface in a gas medium.

$$\ln \frac{P}{P_0} = \frac{-\gamma * V_L * \cos\theta}{r_K * RT} \qquad [3]$$

where P is the vapor pressure, P_0 is the saturated vapor pressure (equilibrium pressure of a flat liquid surface), γ is the surface tension, V_L is the molar volume of the liquid, θ is the contact angle, r_K is the radius of droplet, R is the universal gas constant, and T is the absolute temperature (K).

As the size of liquid droplet decreases, the curvature of the surface and the vapor pressure increase. This equation is based on the thermodynamic principle and does not correlate to the special properties of materials. Therefore, this equation can also theoretically explain the solubilization process, the transferring of molecules from a solid phase to a liquid phase. When the saturated status of a substance is reached, the equilibrium of molecules dissolving and molecules recrystallizing exists. The equilibrium can be destroyed and shifted toward dissolution once the dissolution pressure is increased due to the decreased particle size and increased curvature. Therefore, the saturation solubility is enhanced.

Furthermore, the Ostwald-Freundlich equation indicates that the saturation solubility increases as the particle size decreases.

$$\log\frac{C_s}{C_\alpha} = \frac{2\sigma V}{2.303RT\rho r} \quad [4]$$

where C_s is the saturation solubility, C_α is the solubility of the solid consisting of large particles, σ is the interfacial tension of substance, V is the molar volume of the particle material, R is the gas constant, T is the absolute temperature, ρ is the density of the solid, r is the particle radius.

Müller and Akkar did some experiments to prove that only a slight increase of dissolution pressure was observed for a reduction of drug particle size to 2.0 μm. However, an obvious noteworthy increase of dissolution pressure was detected as the particle size changed from 200 nm to 100 nm. They also pointed out that the increase of dissolution pressure is exponential due to the size reduction (Müller and Akkar 2004).

In the generation of nanocrystals the specific surface area of drug substance is increased and the diffusional distance is decreased because of the fast movement of nanosized particles. According to Noyes-Whitney equation, the enlarged surface area, decreased diffusional distance and the increased saturation solubility all contribute to the enhanced dissolution rate (Moschwitzer and Müller 2006). Furthermore, the improved saturation solubility causes increased drug absorption by passive diffusion from the gut lumen to blood due to the increase of concentration gradient.

The company Nanosystems first introduced nanocrystals to improve the oral bioavailability of poorly water-soluble drugs. Nanosuspension is a system where nanocrystals are dispersed in a liquid media with surfactant or polymer as stabilizing agent (Niwa and Danjo 2013). Technologies developed to produce drug nanocrystal suspensions can be classified as bottom-up technologies, top-down technologies, and combinational technologies.

Bottom-up technology starts from a drug molecule solution and ends with the drug nanoparticles. The drug is dissolved in a solvent first, followed by a precipitation in a non-solvent. Adding stabilizer like surfactants maintains the structure of the nanoparticles. This classical precipitation process was named as “via humida paratum” (v.h.p) (Heinz and Martin 1988). The so-called “hydrosol” method developed around 1980 by Sucker was considered the first example of bottom-up technology. However, the high cost for eliminating the organic solvents used in this process limited the development of this technology in pharmaceutical industry (de Waard, Hinrichs et al. 2008; Junghanns and Müller 2008; de Waard, Grasmeijer et al. 2009).

The top-down technology is a diminution process of large crystals in micrometer range to nanodimensions, by using bead milling or high-pressure homogenization. In the milling method, wet bead milling is usually applied for the advantage of efficient diminution power compared to dry milling (Junyaprasert and Morakul 2015). Wet bead milling is known to be a low-energy process. Drug suspension containing stabilizer and milling media is charged into the milling chamber, where the drug particles are broken down by generated shear force and the collision among milling beads during the

process. The milling technique has been proven to be an important industrially used technology to generate nano products (Keck and Müller 2006; Yuminoki, Seko et al. 2014). Five FDA-approved nanocrystal formulation drugs, Rapamune®, Emend®, Tricor®, Invega® and Megace ES®, are all produced by using this technology. Rapamune® was the first sirolimus nanocrystal product that was introduced to the market by Wyeth in 2000. Compared with sirolimus solution, Rapamune® performed with 21% higher bioavailability due to the improved solubility in aqueous media. Emend® was introduced by Merck the following year, in which aprepitant nanocrytsals were incorporated into pellets and filled in a hard gelatin capsule.

High-pressure homogenization as a high energy inputting process can be performed by two different equipments: microfluidizers and piston-gap homogenizers. In microfluidization, a jet stream with ultra-high speed passes through a "Y" or "Z" interaction chamber, the drug particles are broken into nano-dimension by collision and shear force (Müller and Akkar 2004). The disadvantage of this method is that a relatively high number of cycles are required to get the ideal size of nanocrystals. Piston-gap homogenization is an idea based on the law of Bernoulli. In this process a drug suspended in an aqueous medium is forced by a piston to pass through a tiny homogenization gap with high pressure. Bernoulli's principle is derived from the principle of the conservation of energy. It states that the sum of all forms of energy is the same on all streamlines when a fluid is flowing out from a reservoir because the energy per unit volume in a reservoir is the same everywhere. The energy includes dynamic energy and static energy. The dynamic pressure increases and the static pressure decreases when the liquid goes to through the tiny homogenization gap. At room temperature, when the static pressure equals to the vapor pressure the liquid boils and the gas bubbles generate. Therefore, when the drug nanosuspension goes through the tiny gap and into a normal air condition, the gas bubbles implode immediately, generating nanoparticles (Keck and Müller 2006).

Besides bead milling and high-pressure homogenization technologies, combinational technologies were developed via comprising a pre-treatment of drug suspensions

followed by a high energy process. It was proven that the combinational technologies could accelerate the production process or generate smaller nanocrystals (Moschwitzer and Müller 2006). Baxter introduced the NanoEdge^{TM} technology, which includes a precipitation step and a high pressure homogenization step (James E. Kipp, Joseph Chung Tak Wong et al. 2000). SmartCrystal^{TM} is another combinational technology that can reduce the number of passes through the homogenizer to produce nanocrystals below 100 nm by pretreating the suspension applying bead milling technology (Müller and Keck 2008; Al Shaal, Müller et al. 2010).

Recently, more and more products with nanocrystals are getting on the market. Many efforts have been devoted to manufacturing a solid dosage form from nanosuspension for the obvious advantages of oral dosage form and its high market potential. Coating of a drug nanosuspension into core tablets or into pellets can be performed through film coating or fluidized bed coating. However, it is a time consuming method for high dose products (Luo, Xu et al. 2013). Alternatively, lyophilization and spray drying can convert nanosuspension into a powder form, which can be subsequently used in solid dosage form (Thombre, Shah et al. 2012; De Smet, Saerens et al. 2014; Kumar, Gokhale et al. 2014). Compared with lyophilization, which is a high energy and time consuming process, spray drying can be a more economic technology for the solidification of nanosuspensions. Additionally, another advantage of powders formed through spray drying is better flowability, which is desirable for the production of drugs in solid dosage form.

1.3 Solid dispersion for oral delivery

Solid dispersion is another promising method to improve the oral bioavailability of poorly water-soluble drugs. This method creates a molecular mixture of poorly soluble drugs in hydrophilic carriers. The drugs aqueous solubility and release profile depend on the carrier and the solid dispersion particle properties (Vasconcelos, Sarmento et al. 2007).

With the generation of proper solid dispersions, drug particles can be obtained with reduced particle size (Leuner and Dressman 2000; Bikiaris, Papageorgiou et al. 2005), improved wettability (Karavas, Ktistis et al. 2006), higher porosity (Vasconcelos; and Costa 2007) or an amorphous state (Lloyd, Craig et al. 1999).

According to the characteristics of carriers, solid dispersion can be divided into three generations. Crystalline solid dispersion is the first generation of solid dispersion. It employs crystalline carriers, e.g. urea and sugars，during production (Kanig 1964; Sekiguchi, Ueda et al. 1964; Goldberg, Gibaldi et al. 1966; Goldberg, Gibaldi et al. 1966). In 1960s, Levy and Kanig developed solid dispersion called solid solution for the molecular dispersion containing mannitol as the carrier (Kanig 1964; Sekiguchi, Ueda et al. 1964).

Compared with crystalline material, substances in amorphous state possess high free energy. These substances have a high potential to improve the solubility of poorly soluble drugs. Therefore, the amorphous carriers, usually polymers, were employed to prepare the second and third generations of solid dispersions, both of which can be defined as amorphous solid dispersion. In this case, the drug molecules are dispersed in an irregular form in amorphous carriers (Vilhelmsen, Eliasen et al. 2005; Urbanetz 2006). Two different types of polymers, synthetic polymers and natural product-based polymers, are used in the second generation of solid dispersion. Povidone (PVP) (Worku, Aarts et al. 2014; Puncochova, Ewing et al. 2015) and polyethyleneglycol (PEG) (Guyot, Fawaz et al. 1995; Yao, Bai et al. 2005) are the most commonly used synthetic polymers. Polymers composed by cellulose derivatives, like hydroxypropylmethylcellulose (HPMC) (Mahmah, Tabbakh et al. 2014; Ahuja, Jena et al. 2015), ethylcellulose (Ohara, Kitamura et al. 2005; Desai, Alexander et al. 2006), hydroxypropycellulose (Tanaka, Imai et al. 2006) or starch derivatives (cyclodextrins) (Rodier, Lochard et al. 2005) are defined as the natural carriers.

To improve the dissolution rate of a drug, surfactant carrier or a mixture of carrier and surfactant is employed in the third generation of solid dispersion. In this case, the carriers with surface activity facilitate the dispersion of drug molecules. The surfactants

include inulin (van Drooge, Hinrichs et al. 2006), inutec SPI (Van den Mooter, Weuts et al. 2006), gelucire (Yuksel, Karatas et al. 2003) and poloxamer (Majerik, Charbit et al. 2007) .

Based on the molecular interactions of drugs and carriers, amorphous solid dispersion can be distinguished as solid solution, solid dispersion or a mixture of both. In solid solution drugs are molecularly distributed in an amorphous carrier. This kind of solid dispersion is homogeneous on a molecular level. Amorphous solid suspension occurs when the drug is poorly soluble in a carrier or has an extremely high melting point, in which two phases are exist. Two properties are present in the mixed solid dispersion (Goldberg, Gibaldi et al. 1966; Chiou and Riegelman 1971). The miscibility of drug and carrier and the preparation method both influence the resulting type of solid dispersion (Breitenbach, Schrof et al. 1999).

Melting and solvent evaporation processes are two different ways to generate solid dispersion. The melting method incorporates drug into the carrier in a molten state, followed by cooling and pulverization. However, it was proven that during the process some drugs degraded under the high temperature and also the drug and carrier performed an incomplete miscibility due to the high viscosity of polymeric carrier in the molten state. To overcome the limitations of the melting method, additional technologies were introduced, including hot extrusion, Meltrex™ and melt agglomeration. Hot extrusion is the most commonly used technology consisting of an extrusion process of the mixed drug and carrier at a high rotational speed, and the product is subsequently milled after cooling down (Mahmah, Tabbakh et al. 2014). Kaletra® was manufactured by Abbott Laboratories using the hot melt extrusion method. Two drugs (lopinavir/ritonavir) were dispersed in polyvinylpyrrolidone/vinyl acetate (PVP/VA) to generate the solid dispersion, and the final product was given by capsule. Onmel® announced by Merz, Inc. as another product approved by the FDA was generated by using the hot melt extrusion process, which consists of itraconazole dispersed in HPMC.

The solvent evaporation method includes two steps: the dissolving or suspending of drug and carrier in solvent and the removal of the solvent. Spray drying as one of the most popular drying methods is a good choice to be applied in the solvent evaporation method to produce solid dispersion (Tran, Poudel et al. 2013). Early in 1992, Janssen manufactured Sporanox® capsule by the spray drying method, which included itraconazole as the active ingredient dispersed in HPMC. In 2012, Vertex announced the FDA approval of Kalydeco®. In Kalydeco®, hypromellose acetate succinate (HPMCAS) was used as the polymer to disperse ivacaftor by using spray drying (Huang and Dai 2014).

Although amorphous solid dispersions can improve drugs bioavailability by changing their water solubility, recrystallization is still the major disadvantage. It has the tendency to be in a more stable state during the production or storage due to the temperature and humidity stress.

1.4 Generation of amorphous state in porous material

Amorphous compounds exhibit short-range order over a few molecular dimensions and have physical properties quite different from those of their corresponding crystalline states. They do not possess a well-defined molecular order in their arrangement. According to the special structure property, amorphous compounds can be produced in conditions when precipitation is kinetically faster than crystallization or the disorder of drug molecular during dispersing process, like nanonization or solid dispersion (Auweter H and Bohn H 2002 ; Puncochova, Heng et al. 2014). As the most water-soluble state of drug substances, the amorphous form has the lowest stability attributed to the highest free energy and lowest melting point (Junyaprasert and Morakul 2015). Therefore, although it can reach a higher bioavailability, compared to crystalline compound the potential recrystallization of amorphous compound is still crucial for process development.

Because molecular mobility in high free energy leads to the recrystallization, caging amorphous drugs in tiny space can be a smart idea to prevent the recrystallization. Due

to the special characteristics, like large surface area, tiny pores and large pore volume, porous material can be used to adsorb drug molecules in the amorphous state. Different pore sizes can result in different characteristic adsorption behaviors and physical stabilities. Therefore, porous materials are classified into three types according to their pore sizes. According to the definition of the International Union of Pure and Applied Chemistry (IUPAC): macroporous materials have pore diameters greater than 50 nm, microporous materials have pore diameters less than 2 nm, and mesoporous porous materials thus lies in the middle (Sing, Everett et al. 1985). In the macroporous range, the pores are so wide that they behave like flat surfaces. Whereas in the microporous range, the adsorption potential of wall on each side overlap due to the proximity of walls (Qian and Bogner 2012). Mesoporous materials have a more optimal pore size range. Therefore they have been considered and employed as a potential amorphous drug delivery system to improve oral bioavailability in recent years. Drug adsorption in mesopores depends not only on the wall attraction, but also the interaction between the adsorbate molecules.

Generally, mesoporous materials are derived from molecular assemblies of surfactants. (Kresge, Leonowicz et al. 1992; Zhao, Feng et al. 1998). After the removal of surfactants, mesoporous matrices are obtained with unique features: tiny pores with nano-sized diameter, ordered pore networks, high pore volumes and large surface areas. These characteristics make mesoporous material an ideal candidate to improve the bioavailability of poorly water soluble drugs and control drug delivery systems.

Different mechanisms are introduced for the encapsulation of amorphous drugs in mesoporous materials. First, drugs can be encapsulated into mesopores via the capillarity effect. Mesoporous material is like a sponge structure with a large amount of tiny pores, adsorbing drugs via different states, including solution-phase, melting-phase, even solid-phase. Second, the large internal surface area helps drug adsorption (Prestidge, Barnes et al. 2007). High surface free energy caused by large surface area is transferred to lower free energy state by adsorbing drug molecules (Laitinen, Lobmann et al. 2013). Last but not least, the spatial-constraint effect and decreased free energy

limit the mobility of drug molecules in mesopores. Therefore, the nucleation and crystal growth are avoided. This not only allows the generation of amorphous drug but also contributes to the improvement of formulation stability during shelf time (Qian and Bogner 2012).

The methods for incorporating drugs in porous material can be classified in two ways: solvent and non-solvent. Mostly organic solvents are used in the solvent method. The non-solvent methods include, e.g. the super-critical CO_2 (SC-CO2) method, the melting method, the co-grinding method and the sublimation mass-transfer method.

In the solvent method, a poorly water-soluble drug is dissolved first in a proper organic solvent to generate a concentrated solution. Followed by a wetness impregnation method (Ahern, Hanrahan et al. 2013; Manoj Goyal 2013) or solution immersing method (Vadia and Rajput 2012; Tarique Meer 2013), drug is incorporated into the pores. In the immersion method, porous material is suspended in drug solution with stirring or ultrasound to reach the equilibration of adsorption, followed by the separation of solid from the system using filtration or centrifugation. In the wetness impregnation method, drug solution is added drop-wise on the carrier with gentle stirring, and the added solvent is eliminated afterwards. This process can be repeated several times until the desired drug loading is achieved (Vadher, Parikh et al. 2009).

Based on the solvent method, the developed system encapsulating drugs in the amorphous state was named as CapsMorph® by PharmaSol GmbH Berlin. Gonzalez Ferreiro and Dunmann patented the generation of amorphous itraconazole by loading of Neusilin (Gonzalez Ferreiro, Dunmann et al. 2009). 500 mg itraconazole was dissolved in 2.5 ml of dichloromethane to prepare the solution, which was then added drop-wise to 2.5 g of Neusilin® US under permanent mixing. The solvent was removed using a rotary evaporator. X-ray powder diffraction was performed to analyze the formulation, and no crystalline drug was observed.

In the SC-CO_2 method, drug and porous material are mixed first with or without adsorption enhancer in a closed system with SC-CO_2 for a fixed time under stirring to

make drug dissolved and adsorbed completely, then with a gradual pressure decrease CO_2 is evaporated from the system and the precipitation of drug in porous material is obtained (Ahern, Hanrahan et al. 2013; Li-Hong, Xin et al. 2013).

In the melting method, drug is melted and added to a porous carrier with a specified time of mixing. After a uniform adsorption, the system is cooled, granulated and sieved to obtain drug-loaded granules. (Shrivastava, Ursekar et al. 2009; Aerts, Verraedt et al. 2010). However, the melting method may not reach a high loading capacity of porous material because the high viscosity of the melts can prevent drug from penetrating into the deeper spaces in the pores.

The co-grinding method (Gupta, Vanwert et al. 2003; Madieh, Simone et al. 2007) mixes the drug powder and carrier powder by grinding. The generation of amorphous compound is due to the formation of H-bonds between the drug molecules and carrier, which can spontaneously prevent the crystallization of the drug. This method introduced a different view on the use of porous material (especially silica-based) to produce amorphous drugs. This method is cost-effective and solvent-free, but the drug loading is relatively low.

According to the definition, sublimation is the transition of a substance directly from the solid to the gas phase without passing through the liquid phase. Sublimation occurs when temperature and pressure are below a substance's triple point in its phase diagram (Qian, Suib et al. 2011). The sublimation mass-transfer method is very innovative and simple, but very time-consuming and the drug loading is very low.

Typical mesoporous materials include some types of silica and alumina. Neusilin® US2 developed by Fuji Chemical 1954 is a synthetic amorphous form of magnesium aluminometasilicate. It possesses a specific surface area of 300 m^2/g, particle size of 100 μm and pore size of 15 nm, which all contribute to the potential of drug molecules adsorption. With other exceptional excipient properties, Neusilin® US2 can be used in both direct compression and wet granulation of the solid dosage form. Moreover, it is an accepted safe excipient by the US pharmacopeia and Japanese Pharmaceutical

Codex for no reports of adverse reaction (Gupta, Vanwert et al. 2003; Vadher, Parikh et al. 2009; Müller, Wei et al. 2013).

AEROPERL® 300 Pharma, introduced by Evonik Industries, is an inert amorphous granulated colloidal silicon dioxide. It approximately has a pore volume of 1.6 ml/g and particle size of 30-40 μm, with a high specific surface area of 300 m^2/g. AEROPERL® 300 Pharma has a high absorption capacity for liquids due to its mesoporous particle structure. In addition, it also can be easily used in tableting and capsule filling processes due to the good flowability of its spherical shape (Tarique Meer 2013).

Syloid® mesoporous silica from Grace may also be an intelligent choice for many pharmaceutical formulations due to its unique morphology. Compared with other mesoporous materials, Syloid® is finer sized silica (Kinnari, Makila et al. 2011; Mehanna, Motawaa et al. 2011).

Formac pharmaceuticals cooperated with Grace in 2011 and announced the generation of another mesoporous material SilSol*TM* 6 several years later. SilSol*TM* 6 was developed for optimum pore size and pore size-distribution for amorphization, supersaturation and stability improvement for BCS 2 compounds.

In the future, the development and launch of new porous materials will give pharmaceutical development scientists a panel of options in the field of porous materials generated for amorphous drug delivery.

1.5 Aims of the thesis

The study in this thesis aimed to improve the bioavailability of poorly water-soluble drugs by generating nanocrystal and amorphous formulations:

1. Generation of amorphous hesperidin by loading into mesoporous silica material

AEROPERL® 300 Pharma as an inert amorphous granulated colloidal silicon dioxide has a large pore volume and high specific surface area due to its mesoporous structure.

The aim was to generate amorphous hesperidin for oral delivery and prevent the recrystallization during production or shelf time, by encapsulating hesperidin molecules in the mesopores of AEROPERL® 300 Pharma. The characterization of amorphous formulation was studied in terms of the drug solid state (X-ray diffraction, differential scanning calorimetry), saturation solubility and *in-vitro* release, and compared to the nanocrystal formulation.

2. Controlled release of poorly water-soluble drugs by verifying the drug loading in porous material

The pore size, large surface area and pore volume of mesoporous material play different roles in drug loading process and drug release. The aim was to understand the mechanism of drug loading process and measure the maximum drug loading capacity of AEROPERL® 300 Pharma by using the wetness impregnation method. In addition, when different times of drug loading processes were applied, amorphous hesperidin formulations with different drug loading degrees were obtained to control the *in-vitro* drug release.

3. Characterization of CapsMorph® rutin tablet and comparison with market tablet

Rutin, with a high potential to perform as a drug or nutraceutical, possesses a low oral bioavailability due to the poor solubility in water. The aim was to formulate amorphous rutin by CapsMorph® to improve the saturation solubility. The characterization of rutin CapsMorph® tablet was studied and compared with the market rutin tablet.

4. Development of solid nanocrystals using spray drying technology according to the DoE

In order to improve alternatively the oral bioavailability of hesperidin, nanosuspension stabilized by poloxamer 188 was produced via the wet bead milling process first, followed by a solidification process achieved via spray drying. MODDE 9 was utilized as the DoE tool to design and analyze the spray drying. The influence of spray drying process and protectant (PVP K25) on the particles size of solid nanocrystals was recognized and the best combination of experiment parameters for generating ideal

solid hesperidin nanocrystals was obtained.

1.6 References

Aerts, C. A., E. Verraedt, et al. (2010). "Potential of amorphous microporous silica for ibuprofen controlled release." Int J Pharm **397**(1-2): 84-91.

Ahern, R. J., J. P. Hanrahan, et al. (2013). "Comparison of fenofibrate-mesoporous silica drug-loading processes for enhanced drug delivery." Eur J Pharm Sci **50**(3-4): 400-409.

Ahuja, B. K., S. K. Jena, et al. (2015). "Formulation, optimization and in vitro-in vivo evaluation of febuxostat nanosuspension." Int J Pharm **478**(2): 540-552.

Al Shaal, L., R. H. Müller, et al. (2010). "smartCrystal combination technology - scale up from lab to pilot scale and long term stability." Pharmazie **65**(12): 877-884.

Amidon, G. L., H. Lennernas, et al. (1995). "A Theoretical Basis for a Biopharmaceutic Drug Classification - the Correlation of in-Vitro Drug Product Dissolution and in-Vivo Bioavailability." Pharm Res **12**(3): 413-420.

Auweter H and Bohn H (2002). "Precipitated water-insoluble colorants in colloid disperse." United States Patent **US 6,494,924 B1**

Bikiaris, D., G. Z. Papageorgiou, et al. (2005). "Physicochemical studies on solid dispersions of poorly water-soluble drugs - Evaluation of capabilities and limitations of thermal analysis techniques." Thermochimica Acta **439**(1-2): 58-67.

Breitenbach, J., W. Schrof, et al. (1999). "Confocal Raman-spectroscopy: analytical approach to solid dispersions and mapping of drugs." Pharm Res **16**(7): 1109-1113.

Brough, C. and R. O. Williams, 3rd (2013). "Amorphous solid dispersions and nano-crystal technologies for poorly water-soluble drug delivery." Int J Pharm **453**(1): 157-166.

Chiou, W. L. and S. Riegelman (1971). "Pharmaceutical applications of solid

dispersion systems." J Pharm Sci **60**(9): 1281-1302.

De Smet, L., L. Saerens, et al. (2014). "Formulation of itraconazole nanococrystals and evaluation of their bioavailability in dogs." Eur J Pharm Biopharm **87**(1): 107-113.

de Waard, H., N. Grasmeijer, et al. (2009). "Preparation of drug nanocrystals by controlled crystallization: Application of a 3-way nozzle to prevent premature crystallization for large scale production." Eur J Pharm Sci **38**(3): 224-229.

de Waard, H., W. L. J. Hinrichs, et al. (2008). "A novel bottom-up process to produce drug nanocrystals: Controlled crystallization during freeze-drying." J Control Release **128**(2): 179-183.

Desai, J., K. Alexander, et al. (2006). "Characterization of polymeric dispersions of dimenhydrinate in ethyl cellulose for controlled release." Int J Pharm **308**(1-2): 115-123.

Goldberg, A. H., M. Gibaldi, et al. (1966). "Increasing Dissolution Rates and Gastrointestinal Absorption of Drugs Via Solid Solutions and Eutectic Mixtures .2. Experimental Evaluation of a Eutectic Mixture - Urea-Acetaminophen System." J Pharm Sci **55**(5): 482-&.

Goldberg, A. H., M. Gibaldi, et al. (1966). "Increasing Dissolution Rates and Gastrointestinal Absorption of Drugs Via Solid Solutions and Eutectic Mixtures .4. Chloramphenicol-Urea System." J Pharm Sci **55**(6): 581-&.

Gonzalez Ferreiro, M., C. Dunmann, et al. (2009). "Stabilization of amorphous drugs using sponge-like carrier matrices." European Patent Application. **EP2135601A1**.

Gupta, M. K., A. Vanwert, et al. (2003). "Formation of physically stable amorphous drugs by milling with Neusilin." J Pharm Sci **92**(3): 536-551.

Guyot, M., F. Fawaz, et al. (1995). "Physicochemical Characterization and Dissolution of Norfloxacin/Cyclodextrin Inclusion-Compounds and Peg Solid Dispersions." Int J Pharm **123**(1): 53-63.

Heinz, S. and L. Martin (1988). "Pharmaceutical colloidal hydrosols for injection." UK Patent Application. **2200048**.

Horter, D. and J. B. Dressman (2001). "Influence of physicochemical properties on dissolution of drugs in the gastrointestinal tract." Adv Drug Deliv Rev **46**(1-3): 75-87.

Huang, Y. and W. G. Dai (2014). "Fundamental aspects of solid dispersion technology for poorly soluble drugs." Acta Pharm Sin B **4**(1): 18-25.

James E. Kipp, Joseph Chung Tak Wong, et al. (2000). "Microprecipitation method for preparing submicron suspensions." US Patent. **US7037528 B2**.

Jones, O. A., N. Voulvoulis, et al. (2001). "Human pharmaceuticals in the aquatic environment a review." Environ Technol **22**(12): 1383-1394.

Junghanns, J.-U. A. and R. H. Müller (2008). "Nanocrystal technology, drug delivery and clinical applications." Int J Nanomedicine **3**: 295-309.

Junyaprasert, V. B. and B. Morakul (2015). "Nanocrystals for enhancement of oral bioavailability of poorly water-soluble drugs." Asian J Pharm Sci **10**(1): 13-23.

Kanig, J. L. (1964). "Properties of Fused Mannitol in Compressed Tablets." J Pharm Sci **53**(2): 188-&.

Karavas, E., G. Ktistis, et al. (2006). "Effect of hydrogen bonding interactions on the release mechanism of felodipine from nanodispersions with polyvinylpyrrolidone." Eur J Pharm Biopharm **63**(2): 103-114.

Kawabata, Y., K. Wada, et al. (2011). "Formulation design for poorly water-soluble drugs based on biopharmaceutics classification system: Basic approaches and practical applications." Int J Pharm **420**(1): 1-10.

Keck, C. M. and R. H. Müller (2006). "Drug nanocrystals of poorly soluble drugs produced by high pressure homogenisation." Eur J Pharm Biopharm **62**(1): 3-16.

Keck, C. M. and R. H. Müller (2010). "SmartCrystals: a review of the second generation of drug nanocrystal." Handbook of materials for nanomedicine, Singapore:

Pan Stanford**:** 555-580.

Kinnari, P., E. Makila, et al. (2011). "Comparison of mesoporous silicon and non-ordered mesoporous silica materials as drug carriers for itraconazole." Int J Pharm **414**(1-2): 148-156.

Kresge, C. T., M. E. Leonowicz, et al. (1992). "Ordered Mesoporous Molecular-Sieves Synthesized by a Liquid-Crystal Template Mechanism." Nature **359**(6397): 710-712.

Krishnaiah, Y. S. R. (2010). "Pharmaceutical technologies for enhancing oral bioavailability of poorly soluble drugs." J Bioequiv Availab **2**(2): 028-036.

Kumar, S., R. Gokhale, et al. (2014). "Sugars as bulking agents to prevent nano-crystal aggregation during spray or freeze-drying." Int J Pharm **471**(1-2): 303-311.

Kummerer, K. (2001). "Drugs in the environment: emission of drugs, diagnostic aids and disinfectants into wastewater by hospitals in relation to other sources - a review." Chemosphere **45**(6-7): 957-969.

Laitinen, R., K. Lobmann, et al. (2013). "Emerging trends in the stabilization of amorphous drugs." Int J Pharm **453**(1): 65-79.

Leuner, C. and J. Dressman (2000). "Improving drug solubility for oral delivery using solid dispersions." Eur J Pharm Biopharm **50**(1): 47-60.

Li-Hong, W., C. Xin, et al. (2013). "A novel strategy to design sustained-release poorly water-soluble drug mesoporous silica microparticles based on supercritical fluid technique." Int J Pharm **454**(1): 135-142.

Lloyd, G. R., D. Q. M. Craig, et al. (1999). "A calorimetric investigation into the interaction between paracetamol and polyethlene glycol 4000 in physical mixes and solid dispersions." Eur J Pharm Biopharm **48**(1): 59-65.

Luo, Y., L. Xu, et al. (2013). "Preparation, characterization, stability and in vitro-in vivo evaluation of pellet-layered Simvastatin nanosuspensions." Drug Dev Ind Pharm **39**(7): 936-946.

Madieh, S., M. Simone, et al. (2007). "Investigation of drug-porous adsorbent interactions in drug mixtures with selected porous adsorbents." J Pharm Sci **96**(4): 851-863.

Mahmah, O., R. Tabbakh, et al. (2014). "A comparative study of the effect of spray drying and hot-melt extrusion on the properties of amorphous solid dispersions containing felodipine." J Pharm Pharmacol **66**(2): 275-284.

Majerik, V., G. Charbit, et al. (2007). "Bioavailability enhancement of an active substance by supercritical antisolvent precipitation." J Supercrit Fluids **40**(1): 101-110.

Manoj Goyal, N. P. (2013). "Preparation and Characterization of Solid Dispersion of Itraconazole." J Pharm Sci Innov **2**(5): 23-28.

Mehanna, M. M., A. M. Motawaa, et al. (2011). "Tadalafil inclusion in microporous silica as effective dissolution enhancer: optimization of loading procedure and molecular state characterization." J Pharm Sci **100**(5): 1805-1818.

Merisko-Liversidge, E., G. G. Liversidge, et al. (2003). "Nanocrystal drug particles: Resolving pharmaceutical formulation issues associated with poorly water-soluble compounds." Abstracts of Papers of the American Chemical Society **226**: U528-U528.

Moschwitzer, J. and R. H. Müller (2006). "New method for the effective production of ultrafine drug nanocrystals." J Nanosci Nanotechnol **6**(9-10): 3145-3153.

Müller, R. H. and A. Akkar (2004). "Drug Nanocrystals of Poorly Soluble Drugs." Encyclopedia of Nanoscience and Nanotechnology. H. S. Nalwa, American Scientific Publishers. **2:** 627-638.

Müller, R. H., S. Gohla, et al. (2011). "State of the art of nanocrystals--special features, production, nanotoxicology aspects and intracellular delivery." Eur J Pharm Biopharm **78**(1): 1-9.

Müller, R. H. and C. M. Keck (2008). "Second generation of drug nanocrystals for delivery of poorly soluble drugs: smartCrystal technology." Eur J Pharm Sci **34**(1): S20-S21.

Müller, R. H., Q. Wei, et al. (2013). "CapsMorph: >4 Years Long-Term Stability of Industrially Feasible Amorphous Drug Formulations." Controlled Release Society. Honolulu, Hawaii, USA.

Niwa, T. and K. Danjo (2013). "Design of self-dispersible dry nanosuspension through wet milling and spray freeze-drying for poorly water-soluble drugs." Eur J Pharm Sci **50**(3-4): 272-281.

Ohara, T., S. Kitamura, et al. (2005). "Dissolution mechanism of poorly water-soluble drug from extended release solid dispersion system with ethylcellulose and hydroxypropylmethylcellulose." Int J Pharm **302**(1-2): 95-102.

Prakash Khadka and J. Ro (2014). "Pharmaceutical particle technologies: An approach to improve drug solubility, dissolution and bioavailability." Asian J Pharm Sci **9**: 304-316.

Prestidge, C. A., T. J. Barnes, et al. (2007). "Mesoporous silicon: a platform for the delivery of therapeutics." Expert Opin Drug Deliv **4**(2): 101-110.

Puncochova, K., A. V. Ewing, et al. (2015). "Identifying the mechanisms of drug release from amorphous solid dispersions using MRI and ATR-FTIR spectroscopic imaging." Int J Pharm **483**(1-2): 256-267.

Puncochova, K., J. Y. Heng, et al. (2014). "Investigation of drug-polymer interaction in solid dispersions by vapour sorption methods." Int J Pharm **469**(1): 159-167.

Qian, K. K. and R. H. Bogner (2012). "Application of mesoporous silicon dioxide and silicate in oral amorphous drug delivery systems." J Pharm Sci **101**(2): 444-463.

Qian, K. K., S. L. Suib, et al. (2011). "Spontaneous crystalline-to-amorphous phase transformation of organic or medicinal compounds in the presence of porous media, part 2: amorphization capacity and mechanisms of interaction." J Pharm Sci **100**(11): 4674-4686.

Rodier, E., H. Lochard, et al. (2005). "A three step supercritical process to improve the dissolution rate of eflucimibe." Eur J Pharm Sci **26**(2): 184-193.

Sakaeda, T., N. Okamura, et al. (2001). "Molecular and pharmacokinetic properties of 222 commercially available oral drugs in humans." Biol Pharm Bull **24**(8): 935-940.

Sekiguchi, K., Y. Ueda, et al. (1964). "Studies on Absorption of Eutectic Mixture .2. Absorption of Fused Conglomerates of Chloramphenicol + Urea in Rabbits." Chem Pharm Bull (Tokyo) **12**(2): 134-+.

Shegokar, R. and R. H. Müller (2010). "Nanocrystals: industrially feasible multifunctional formulation technology for poorly soluble actives." Int J Pharm **399**(1-2): 129-139.

Shrivastava, A. R., B. Ursekar, et al. (2009). "Design, Optimization, Preparation and Evaluation of Dispersion Granules of Valsartan and Formulation into Tablets." Curr Drug Deliv **6**(1): 10.

Sing, K. S. W., D. H. Everett, et al. (1985). "Reporting Physisorption Data for Gas Solid Systems with Special Reference to the Determination of Surface-Area and Porosity (Recommendations 1984)." Pure Appl Chem **57**(4): 603-619.

Stegemann, S., F. Leveiller, et al. (2007). "When poor solubility becomes an issue: From early stage to proof of concept." Eur J Pharm Sci **31**(5): 249-261.

Takagi, T., C. Ramachandran, et al. (2006). "A provisional biopharmaceutical classification of the top 200 oral drug products in the United States, Great Britain, Spain, and Japan." Mol Pharm **3**(6): 631-643.

Tanaka, N., K. Imai, et al. (2006). "Development of novel sustained-release system, disintegration-controlled matrix tablet (DCMT) with solid dispersion granules of nilvadipine (II): In vivo evaluation." J Control Release **112**(1): 51-56.

Tarique Meer, R. F., Deepak Khanna, Purnima Amin (2013). "Solubility modulation of bicalutamide using porous silica." J Pharm Invest **43**: 7.

Ternes, T. A. (1998). "Occurrence of drugs in German sewage treatment plants and rivers." Water Res **32**(11): 3245-3260.

Thombre, A. G., J. C. Shah, et al. (2012). "In vitro and in vivo characterization of amorphous, nanocrystalline, and crystalline ziprasidone formulations." Int J Pharm **428**(1-2): 8-17.

Tran, T. H., B. K. Poudel, et al. (2013). "Development of raloxifene-solid dispersion with improved oral bioavailability via spray-drying technique." Arch Pharm Res **36**(1): 86-93.

Urbanetz, N. A. (2006). "Stabilization of solid dispersions of nimodipine and polyethylene glycol 2000." Eur J Pharm Sci **28**(1-2): 67-76.

Vadher, A. H., J. R. Parikh, et al. (2009). "Preparation and characterization of co-grinded mixtures of aceclofenac and neusilin US2 for dissolution enhancement of aceclofenac." AAPS PharmSciTech **10**(2): 606-614.

Vadia, N. and S. Rajput (2012). "Study on formulation variables of methotrexate loaded mesoporous MCM-41 nanoparticles for dissolution enhancement." Eur J Pharm Sci **45**(1-2): 8-18.

Van den Mooter, G., I. Weuts, et al. (2006). "Evaluation of Inutec SP1 as a new carrier in the formulation of solid dispersions for poorly soluble drugs." Int J Pharm **316**(1-2): 1-6.

van Drooge, D. J., W. L. J. Hinrichs, et al. (2006). "Characterization of the molecular distribution of drugs in glassy solid dispersions at the nano-meter scale, using differential scanning calorimetry and gravimetric water vapour sorption techniques." Int J Pharm **310**(1-2): 220-229.

Vasconcelos, T., B. Sarmento, et al. (2007). "Solid dispersions as strategy to improve oral bioavailability of poor water soluble drugs." Drug Discov Today **12**(23-24): 1068-1075.

Vasconcelos;, T. and P. Costa (2007). "Development of a rapid dissolving ibuprofen solid dispersion." Pharmaceutical Sciences Wolrd Conference.

Vieth, M., M. G. Siegel, et al. (2004). "Characteristic physical properties and structural

fragments of marketed oral drugs." J Med Chem **47**(1): 224-232.

Vilhelmsen, T., H. Eliasen, et al. (2005). "Effect of a melt agglomeration process on agglomerates containing solid dispersions." Int J Pharm **303**(1-2): 132-142.

Williams, H. D., N. L. Trevaskis, et al. (2013). "Strategies to Address Low Drug Solubility in Discovery and Development." Pharmacol Rev **65**(1): 315-499.

Worku, Z. A., J. Aarts, et al. (2014). "Influence of compression forces on the structural stability of naproxen/PVP-VA 64 solid dispersions." Mol Pharm **11**(4): 1102-1108.

Yao, W. W., T. C. Bai, et al. (2005). "Thermodynamic properties for the system of silybin and poly(ethylene glycol) 6000." Thermochimica Acta **437**(1-2): 17-20.

Yu, L. X., G. L. Amidon, et al. (2002). "Biopharmaceutics classification system: The scientific basis for biowaiver extensions." Pharm Res **19**(7): 921-925.

Yuksel, N., A. Karatas, et al. (2003). "Enhanced bioavailability of piroxicam using Gelucire 44/14 and Labrasol: in vitro and in vivo evaluation." Eur J Pharm Biopharm **56**(3): 453-459.

Yuminoki, K., F. Seko, et al. (2014). "Preparation and evaluation of high dispersion stable nanocrystal formulation of poorly water-soluble compounds by using povacoat." J Pharm Sci **103**(11): 3772-3781.

Zhao, D. Y., J. L. Feng, et al. (1998). "Triblock copolymer syntheses of mesoporous silica with periodic 50 to 300 angstrom pores." Science **279**(5350): 548-552.

2 CapsMorph® technology for oral delivery - theory, preparation & characterization

https://doi.org/10.1016/j.ijpharm.2014.10.068 (page 29-38)

Published in: International Journal of Pharmaceutics, Volume 482, Issues 1–2, 30 March 2015, Pages 11–20

3 Oral hesperidin – amorphization & improved dissolution properties by controlled loading onto porous silica

https://doi.org/10.1016/j.ijpharm.2016.11.005 (page 40-50)

Published in: International Journal of Pharmaceutics, Volume 518, Issues 1–2, 25 February 2017, Pages 253–263

4 CapsMorph® technology for generation of long-term stable amorphous rutin in tablets

https://doi.org/10.1016/j.ejpb.2016.11.009 (page 52-62)

Published in: European Journal of Pharmaceutics and Biopharmaceutics, Volume 113, April 2017, Pages 97–107

5 Solidification of hesperidin nanosuspension by spray drying optimized by Design of Experiment (DoE)

(Accepted by Drug Development and Industrial Pharmacy)

Abstract

For final solid dosage forms, aqueous liquid nanosuspensions need to be solidified, whereas spray drying is a large-scale cost-effective industrial process. To accelerate the determination of optimal spray drying parameters, a "Design of Experiment" (DoE) software was applied to produce well re-dispersible hesperidin nanocrystals. A nanosuspension with 18 % (w/w) of hesperidin stabilized by 1% (w/w) of poloxamer 188 was produced by wet bead milling. The sizes of original and re-dispersed spray-dried nanosuspensions were determined by laser diffractometry (LD) and photon correlation spectroscopy (PCS), and used as effect parameters. In addition light microscopy was performed to judge the re-dispersion quality. After a two-step design of MODDE 9, screening model and response surface model (RSM), the inlet temperature of spray dryer and the concentration of protectant (polyvinylpyrrolidone, PVP K25) were identified as the most important factors affecting the re-dispersion of nanocrystals. By a decrease of the inlet temperature and an increase of the concentration of PVP K25, the nanocrystal size could be maintained unchanged. As predicted in the RSM modeling, when 5 % (w/w) of PVP K25 was added in an 18 % (w/w) of hesperidin nanosuspension, subsequently spray dried at an inlet temperature of 100 ^{o}C, well re-dispersed solid nanocrystals with an average particle size of 276 ± 1.98 nm were obtained. By the use of PVP K25, the saturation solubility of the re-dispersed nanocrystals in water was improved to 86.81 ± 1.51 μg/ml, about 2.5-fold of the original nanosuspension. In addition, the dissolution velocity was accelerated. This was attributed to the additional effects of steric stabilization on the nanocrystals and solubilization by the PVP polymer from spray drying. In case nanosuspensions need to be solidified after the wet production, stabilizers such as PVP should be preferred which can act at the same time as protectant in the subsequent spray drying process.

5.1 Introduction

Nanonization, i.e. production of nanocrystals, is an effective method to improve the solubility of poorly water-soluble drugs (Keck and Müller 2006; Junghanns and Müller 2008). According to the Noyes-Whitney equation, when the size of active substances is decreased to a nano size, the dissolution rate (dc/dt) of the drug substance increases due to the increased specific surface area (A) and the decreased diffusional layer (h) (Noyes and Whitney 1897). In addition, based on the Kelvin equation, the kinetic saturation solubility (Cs) increases due to an increased dissolution pressure (Junyaprasert and Morakul 2015). Nanocrystals can be prepared by precipitation, wet bead milling, high pressure homogenization, or combination of these technologies, and are typically obtained from these processes as a fluid nanosuspension, e.g. nanocrystals in aqueous surfactant solution (Kipp 2004; Chaubal and Popescu 2008).

However, being a liquid system, highly dispersed nanosuspensions can show physical instabilities, e.g. crystal growth by Ostwald ripening, phase separation or aggregation. A simple solution is to transfer the nanosuspensions to dry products. Recently, the solidification of nanosuspensions has been performed by coating of nanosuspensions onto core tablets, spray drying or freeze drying (Engers, Teng et al. 2010; Bose, Schenck et al. 2012; Sun, Ni et al. 2014; Zhang, Guan et al. 2014). The obtained products were named “solid nano crystals” (SNCs) having an improved stability. In addition, SNCs can be processed to solid dosage forms, such as tablets, capsules, etc.

Because of a number of advantages in solidifying solutions and suspensions, spray drying is commonly applied in many areas, including pharmaceutics, paint, food, excipient industry and chemistry (Patel, Agrawal et al. 2014). Spray drying has also been utilized to solidify nanosuspensions (Chaubal and Popescu 2008; Van Eerdenbrugh, Froyen et al. 2008). Due to the high surface free energy, nanocrystals are prone to aggregate during spray drying. To solve this problem, different studies have been done (Kumar, Gokhale et al. 2014; Kumar, Xu et al. 2014). Ideal SNCs should be re-dispersed instantaneously in aqueous media without aggregation (Yue, Wang et al.

2015). In the present study design of experiment (DoE) was applied to assess optimal spray drying conditions in a rational, effective way.

Hesperidin was used as a model active with relevance to the market, i.e. being poorly soluble and having oral bioavailability problems. It could be shown, that the dissolution properties of hesperidin nanocrystal tablets were clearly superior to tablets with µm-sized crystals, and also a marketed tablet (Mauludin 2008). Hesperidin as a flavonoid can scavenge reactive oxygen species to prevent biological and chemical substance from oxidative damage, thus to support various disease treatment. However, the low aqueous solubility limits the application of hesperidin in pharmaceutical and nutraceutical field (Scholz and Keck 2014). Therefore, in the present study hesperidin nanosuspension stabilized by poloxamer 188 was produced on a large scale using wet bead milling, followed by spray drying with conditions optimized by DoE.

It is known that the process parameters (inlet temperature, drying gas flow rate, feed rate, nozzle size, compressed air flow rate) of spray dryer and the formulation parameters (feed composition, solid content) both contribute to the response of nanoparticles size (Paudel, Worku et al. 2013). Design of Experiment (DoE) is a common tool to facilitate the determining critical factors that could affect a process or a result in both academia and industry (Kumar, Xu et al. 2014). A MODDE 9 (MODeling and DEsign) software (patented by Umetrics) was used to make a design for the spray drying of nanosuspension. The particle size of the obtained SNCs was the response for choosing the suitable spray drying conditions. In addition, a series of studies were performed to determine the difference in physiochemical characteristics between the nanosuspension and the produced SNCs (saturation solubility, dissolution).

5.2 Materials and methods

5.2.1 Materials

Hesperidin was purchased from DENK Ingredients GmbH (Munich， Germany), Poloxamer 188 (Kolliphor® P 188) was donated by BASF (Ludwigshafen, Germany).

PVP K25 (Kollidon® 25) was purchased from Sigma-Aldrich (St. Louis, USA) and selected as the protectant of nanocrystals in spray drying.

5.2.2 Methods

5.2.2.1 Production of the hesperidin nanosuspension

18% (w/w) of hesperidin was dispersed into 1% (w/w) of poloxamer 188 solution by stirring to obtain the pre-suspension. The pre-suspension was passed through the wet bead mill PML-2 (Bühler, Switzerland) with a milling chamber of 1050 ml. Three-quarters (75%) of the volume was filled with the milling medium, Yttria stabilized zirconium beads with a size of 0.4–0.6 mm (Hosokawa Alpine, Germany). After 5 passages of continuous running (particle size was monitored during the milling) with a rotator speed of 2000 rpm and 10% of pump capacity, the hesperidin nanosuspension was obtained. During the whole process, the temperature of the milling chamber was controlled at 5 °C.

5.2.2.2 Particle shape and size analysis

Light microscope

A light microscope (Leitz Ortophlan, Leitz, Germany) with a CMEX-1 digital camera (Euromex Microscopen BV, Netherlands) was used to detect the potential large particles or agglomerations in nanosuspension. Samples spread gently between the glass slide and cover slide were analyzed at 400 × magnification.

Laser diffractometry (LD)

The particle size distribution of hesperidin nanosuspension was measured by using laser diffractometry (LD). A Mastersizer 2000 (Malvern Instruments, UK) was employed. The selected characterization parameters were the diameters d(v)10%, d(v)50%, d(v)90% and d(v)95%, which were calculated in volume-weighted diameters. A value of d(v)10% means that 10% of the particles in the tested samples are smaller than the given value, and this applies to the other parameters as well. Calculations were

performed using the Mie theory, the refractive index (RI) used was 1.57, and the imaginary refractive index (IRI) was 0.01 (Petersen 2008). The samples were dispersed in water and measured with medium sonication.

Photon correlation spectroscopy (PCS)

A Zetasizer Nano ZS (Malvern Instruments, UK) was used to measure particles between 0.6 nm to 6 μm. The z-average is measured for the mean size of the particles, which is an intensity-weighted mean diameter of the bulk population. The polydispersity index (PI) describes the width of the particle size distribution. All samples were measured 10 subruns in triplicate at 25 ^{o}C to calculate the means and standard deviations.

5.2.2.3 DoE of spray drying

MODDE 9 software was used to design the spray drying of hesperidin nanosuspension. The protectant (PVP K25) concentration, the inlet temperature and the feeding rate of the spray dryer were selected as the varying parameters. The size of re-dispersed spray-dried nanocrystals was measured as the response parameter. In the screening model, the determining factors of the particle size were verified. Then, the best combination of the determining parameters for achieving optimal SNCs was predicted and confirmed in the response surface model (RSM).

5.2.2.4 Re-dispersion of solid nanocrystals

Hesperidin SNCs after spray drying were re-dispersed in water with a gentle shake. Light microscopy was used to check potential agglomeration in the dispersion. PCS and LD were performed to measure the particle size as mentioned above.

5.2.2.5 X-ray diffraction (XRD)

The X-ray diffraction patterns of hesperidin raw material and SNCs were obtained by a Philips X-ray Generator PW 1830 (Philips, Netherlands) at a scattering angle range from 0.6° to 40°. A voltage of 40 kV and a current of 25 mA were applied.

5.2.2.6 Differential scanning calorimetry (DSC)

The thermal analysis was performed for SNCs and compared with that of raw material. Prior to the measurement, samples were weighed accurately (about 3 mg) in aluminum pans with punched covers. Samples were heated from 25 ^{o}C to 300 ^{o}C at a heating rate of 10 ^{o}C/min to collect the heating curves. Nitrogen was used as the purge gas with a flow rate of 20 ml/min.

5.2.2.7 Kinetic saturation solubility

First excess hesperidin raw material, nanosuspension and SNCs were placed in different vials, then 20 ml of dissolution media, water (pH 6.7), 0.1 M hydrochloric acid (HCl) solution and pH 6.8 phosphate buffer saline (PBS), were added respectively. In order to compensate for the influence of PVP K25 on the saturation solubility of SNCs, 5% (w/w) of PVP K25 was added to each medium when hesperidin raw material and nanosuspension were measured. The vials were placed in an Innova 4230 refrigerated incubator shaker (New Brunswick Scientific GmbH, Germany) and were constantly agitated at 100 rpm to achieve a uniform mixing. The temperature was controlled at 37 ^{o}C during the entire measuring process. 2 ml samples from the supernatant were collected after 0.5 h, 1 h, 2 h, 4 h, 6 h, 8 h, 24 h and 48 h. To obtain clear supernatants, samples were centrifuged at 23,000 × g for 40 min at 37 ^{o}C using a Heraeus Biofuge Stratos centrifuge (Thermo Fisher Scientific, Germany). To obtain the mean saturation solubility and standard deviation, each sample was performed in triplicate in each media. The concentrations of hesperidin in the final supernatants were determined by high performance liquid chromatography (HPLC).

5.2.2.8 In-vitro release study

A Pharmatest PTW SIII USP XXIII rotating paddle apparatus (Pharma Test Apparatebau AG, Germany) was used to obtain the dissolution profiles of hesperidin raw material, nanosuspension and hesperidin SNCs. Dissolution tests were conducted at 37 ^{o}C with a rotating speed of 100 rpm in different media, 900 ml of water, 0.1 M HCl solution and pH 6.8 PBS. Samples taken at the specific time intervals were centrifuged

in the same way as described in section 5.2.2.7. After each sampling, the same volume of the test medium was supplemented into the system. In this study, all the samples were measured in triplicate in each medium to calculate the means and standard deviations. HPLC was performed to determine the drug-released concentration at each time point. Considering the drug content in the marketed tablets (50 mg) (Bergan, Schmid-Schonbein et al. 2001; Ramelet 2001), the dissolution test was not performed in sink condition to be closer to the *in vivo* situation with limited volume in the gastrointestinal tract. 50 mg of hesperidin raw material, 277.78 mg of 18% hesperidin nanosuspension (containing 50 mg of hesperidin) and 68.49 mg of hesperidin SNCs (with 5.5% of PVP, containing 50 mg of hesperidin) were added in 900 ml of water, 0.1 M HCl and pH 6.8 PBS, respectively.

5.2.2.9 HPLC analysis

The concentrations of hesperidin in different samples were determined using an HPLC system consisting of a KromaSystem 2000 (Kontron Instruments GmbH, Germany), a solvent delivery pump and a UV detector model 430 (Kontron Instruments SpA, Italy) that measured at 285 nm. A Eurospher 100-5 C18 (4 × 250 mm, 5 µm) was used as the analytical column at 25 °C. The mixture of acetic buffer (pH 4.8) and acetonitrile at a ratio of 75:25 (v/v) was used as the mobile phase at a flow rate of 1 ml/min. The retention time was roughly 7 min.

5.3 Results and discussion

5.3.1 Particle shape and size distribution of nanosuspension

Wet bead milling and high pressure homogenization (HPH) are two frequently used top-down techniques to produce nanocrystals. Most of the products on the market are produced by wet bead milling. Compared with high pressure homogenization, wet bead milling is a low-energy process in which drug particles are broken by generated shear force and collision among milling beads during production (Keck and Müller 2006;

Yuminoki, Seko et al. 2014). The particles of hesperidin in the processed suspension became smaller after each cycle of bead milling and the expected nanoparticle size was obtained after five cycles. Light microscopy (Figure 5-1) shows a very fine dispersion of the obtained hesperidin nanosuspension, no agglomeration could be seen. To increase the probability of detecting even only a few agglomerates, the concentrated nanosuspension was analyzed and not diluted. PCS results showed that the hesperidin nanosuspension possessed an average particle size of 290 ± 2.16 nm, LD results showed that half of the particles were smaller than 0.233 µm (d(v) 50%) and only 5% of the particles were larger than 1.644 µm (d(v) 95%) (Table 5-1). PCS and LD data were well in agreement with light microscopy.

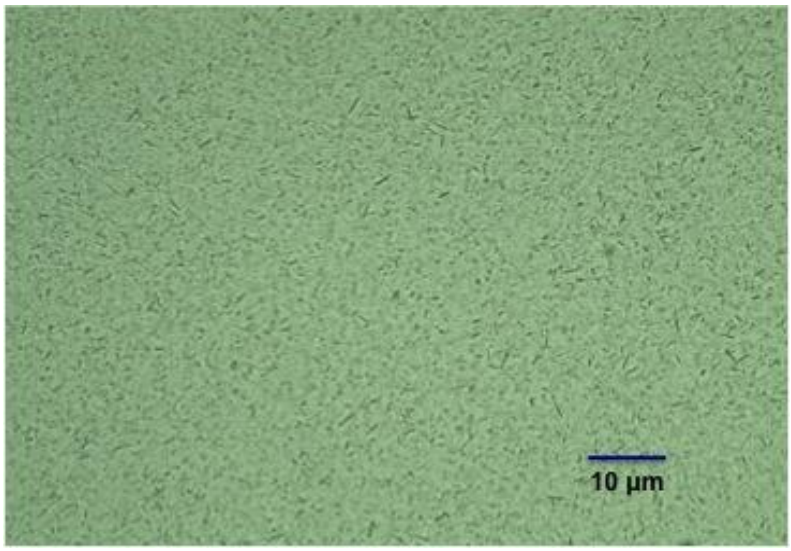

Figure 5-1: Light microscopy picture of hesperidin nanosuspension after five cycles of wet bead milling (magnification 400 ×, scale = 10 µm).

Table 5-1: PCS means with standard deviation (number of parallel samples: n = 3) and LD measurement results of hesperidin nanosuspension after five cycles of wet bead milling (PI = polydispersity index)

	PCS		LD		
hesperidin nanosuspension	z-average (nm)	PI	d(v)50% (µm)	d(v)90% (µm)	d(v)95% (µm)
	290 ± 2.16	0.244 ± 0.002	0.233	0.760	1.644

5.3.2 Design of spray drying

5.3.2.1 Screening model design

The worksheet design and the response

Based on preliminary experiments, the inlet temperature and feeding rate of spray dryer and the protectant (PVP K25) concentration were proven as the important parameters that could affect the size of SNCs. To further verify which factors are the determining factors of particle size and how do they work, the screening model of the MODDE 9 software was performed to design the first step study.

Table 5-2: The worksheet designed by the screening model of MODDE 9 software and the results of LD d(v)50% and PCS size. (Exp No. = experiment number, Con. of PVP = concentration of PVP).

Exp No	Con. of PVP (%)	Inlet temperature (°C)	Feeding rate (ml/min)	Size-LD d(v)50% (µm)	Size-PCS (nm)
1	1.0	100	1.5	0.278	309
2	10.0	100	1.5	0.252	257
3	1.0	140	1.5	1.000	609
4	10.0	140	1.5	0.283	502
5	1.0	100	4.5	0.278	321
6	10.0	100	4.5	0.234	247
7	1.0	140	4.5	1.000	367
8	10.0	140	4.5	0.244	260
9	5.5	120	3.0	0.228	256
10	5.5	120	3.0	0.230	255
11	5.5	120	3.0	0.231	253

The experiment design is listed in Table 5-2. To get a high production efficiency, the 18% (w/w) original hesperidin nanosuspension was employed directly without any dilution. It has been reported that the inlet temperature in the range of 80-150 ^{o}C is used for spray drying nanosuspension (Nekkanti, Pillai et al. 2009; Pilcer, Vanderbist et al. 2009; Mou, Chen et al. 2011). Because a low inlet temperature (lower than 100 ^{o}C) leads to a high residual moisture content in products, and a high inlet temperature causes an excessive collection of particles on the chamber of spray dryer, the inlet temperature of spray dryer was varied from 100 ^{o}C to 140 ^{o}C in this design, as reported previously

(Chaubal and Popescu 2008). The concentration of PVP K25 was increased from 1% to 10% (w/w) and the feeding rate of spray dryer was ranged from 1.5 ml/min to 4.5 ml/min. The sizes of the SNCs after spray drying are listed in Table 5-2 as the response, in terms of LD d(v)50% and PCS respectively.

The LD d(v)50% results revealed a variation of SNCs size from 0.228 μm to 1.000 μm during the changing of operating conditions. When the inlet temperature was increased to 140 ^{o}C and a low concentration of PVP K25 was applied, the obtained SNCs showed large particle sizes, no matter how the feeding rate changed. However, when the inlet temperature was decreased to 120 ^{o}C, a small size of SNCs could be achieved even with a low concentration of PVP K25. As a critical process parameter of spray drying, inlet temperature controls the drying rate of the atomized droplets and the structure of the final product (Cal and Sollohub 2010). With a high inlet temperature, the molecular movement is enhanced to increase the possibility of nanoparticles agglomeration. In addition, PVP K25 (melting point, 130 ^{o}C) can be melted when passing through the spraying nozzle and become sticky under high inlet temperature. Spontaneously it could adhere onto the chamber of the spray dryer together with hesperidin nanoparticles. The minimum production yield was obtained when the highest inlet temperature was applied (data now shown here).

However, it was noticed that increasing the concentration of PVP K25 in the nanosuspension allowed the decrease of SNCs size even at a high inlet temperature. This may be because PVP K25 allows a well dispersion of hesperidin nanoparticles inside a PVP matrix. The smallest SNCs size was obtained by a combination of the parameters: 5.5% (w/w) of PVP K25, inlet temperature of 120 ^{o}C and feeding rate of 3 ml/min.

Similar trends were observed from the PCS results. The smallest particle size (247 nm) was observed in the Exp No 6 when the lowest inlet temperature (100 ^{o}C), the highest PVP K25 concentration (10%, w/w) and the fastest feeding rate (4.5 ml/min) were applied.

The coefficient plots

The coefficient plot through the analysis of LD d(v)50% is presented in Figure 5-2 (A). According to the explanation of the software, the PVP K25 concentration, the inlet temperature and the interplay of the two factors were recognized as the significant model terms in the process. This means that the inlet temperature and the PVP K25 concentration are the determining critical factors in the spray drying process that can directly affect the response of SNCs.

However, in the PCS coefficient plot shown in Figure 5-2 (B), only the inlet temperature was marked as the significant model term.

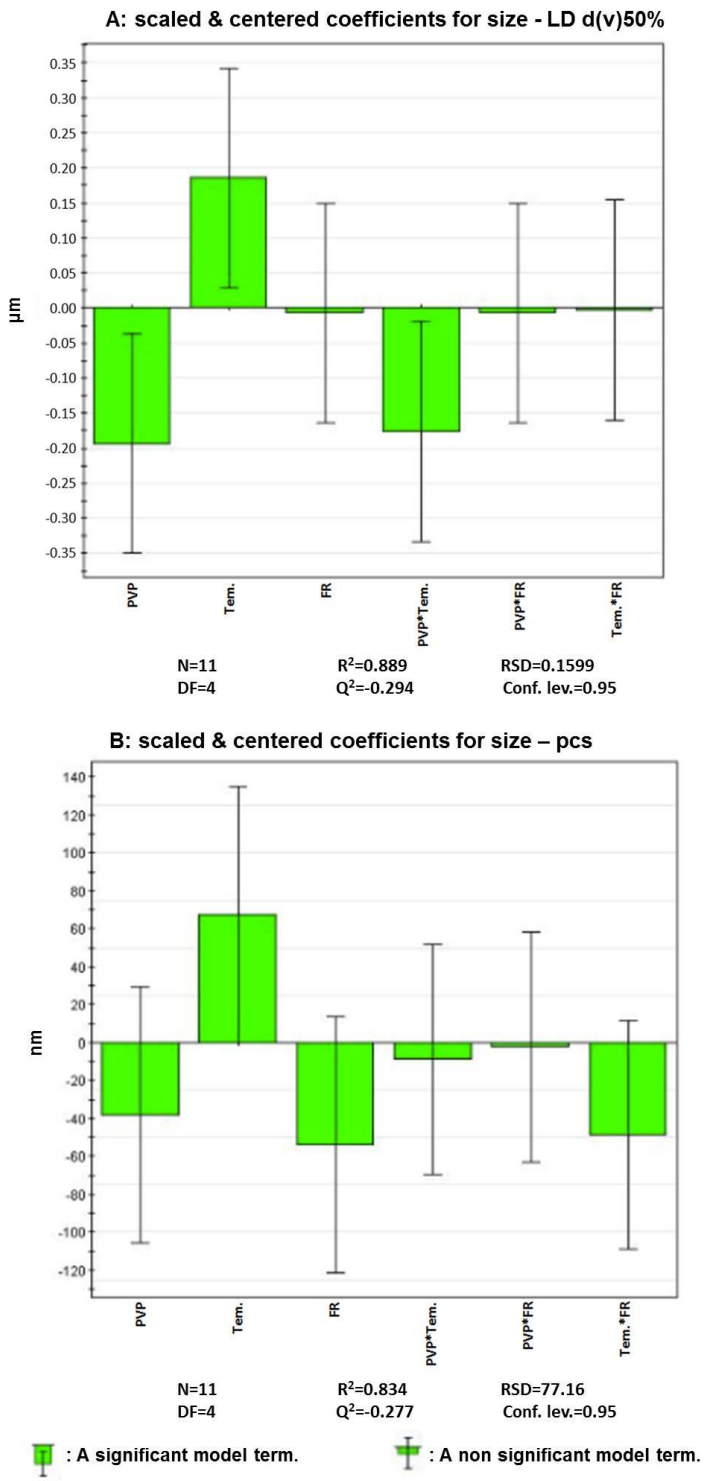

Figure 5-2: The coefficient plots given by the screening model of MODDE 9 software following the analysis of LD d(v)50% (A) and PCS (B) size. PVP = the concentration of PVP, Tem. = the inlet temperature, FR = feeding rate, N = total number of experiments, R^2 = the fraction of the variation of the response explained by the model, RSD = the Residual Standard Deviation, DF = Degree of Freedom, Q^2 = the fraction of the variation of the response predicted by the model according to cross validation, Conf. Lev.= Confidence Level. (The explanation is from the User Guider).

The prediction plots

The prediction plots show how the significant model terms affect the result. As shown in Figure 5-3 (A) for diameter LD d(v)50%, the size of SNCs decreases with increasing concentration of PVP K25 added to the nanosuspension and decrease of inlet temperature. This is in agreement with the LD results and the coefficient plots.

The PCS prediction plot in Figure 5-3 (B) shows that a low inlet temperature allows the reduction of SNCs size.

The upper curve (green) shows the predicted upper limit of SNCs size as the changing of significant model terms. The significant model term(s) are the concentration of PVP and the inlet temperature in graph A, and is the inlet temperature in graph B. Similarly, the middle curve (black) and the lower curve (blue) indicate the predicted mean value and lower limit of SNCs as the changing of significant model terms.

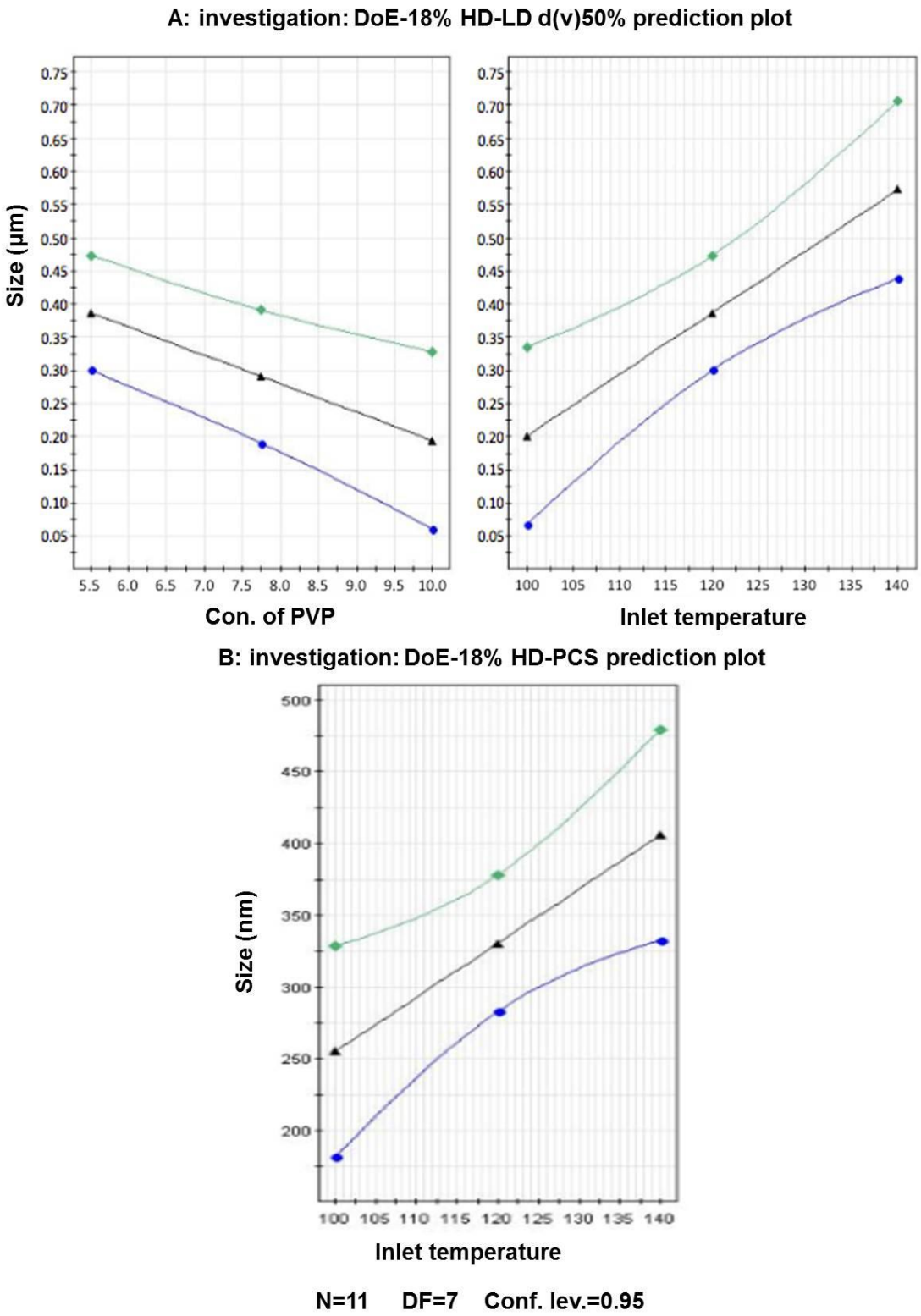

Figure 5-3: The prediction plots given by the screening model of MODDE 9 software following the analysis of LD d(v)50% (A) and PCS size (B) (18% HD = 18% hesperidin concentration in suspension, N = total number of experiments, DF = Degree of Freedom, Conf. lev. = confidence level).

5.3.2.2 Response surface model (RSM) design

The worksheet design and the response

In the previous screening model investigation, the protectant concentration and the inlet temperature were determined as two significant factors that affected the process. Therefore, a response surface model design was made with the two factors to optimize the spray drying process.

Table 5-3：The worksheet designed by the RSM model of MODDE 9 software and the results of LD d(v)50% and PCS size. (Exp No. = Experiment Number, Con. of PVP = Concentration of PVP).

Exp No.	Con. of PVP (%)	Inlet temperature (°C)	Size-LD d(v)50% (μm)	Size-PCS (nm)
1	1.0	100	0.278	321
2	10.0	100	0.234	247
3	1.0	140	0.300	367
4	10.0	140	0.244	285
5	1.0	120	0.297	323
6	10.0	120	0.224	276
7	5.5	100	0.222	266
8	5.5	140	0.253	363
9	5.5	120	0.240	270
10	5.5	120	0.246	278
11	5.5	120	0.245	275

Table 5-3 shows the experiment design under the RSM model and the responses of LD d(v)50% and PCS size. In the result of LD d(v)50% the largest particles were detected when the spray drying was applied at an inlet temperature of 140 ^{o}C and only 1% of PVP K25 was added into the hesperidin nanosuspension. Furthermore, in the result of PCS, when the inlet temperature was decreased to 100 ^{o}C and 10% of PVP K25 was added in the nanosuspension, the SNCs with an average size of 247 nm were obtained. In addition, three different inlet temperatures, 100 ^{o}C, 120 ^{o}C and 140 ^{o}C, were performed to further demonstrate the effect of inlet temperature on SNCs size, while keeping the same moderate protectant concentration. It turned out that the SNCs, which possess an average size of 266 nm and a d(v)50% of 0.222 um, were achieved when the spray drying of nanosuspension was performed at an inlet temperature of 100 ^{o}C and

5.5% of PVP K25 was added as protectant. The corresponding PCS size was 266 nm (i.e. no practical difference to the 247 nm obtained with a higher (10%) PVP K25 concentration). Based on this data, 5.5% of PVP K25 would be sufficient, and 10% has no further improving effect on size.

The contour plots and surface plots

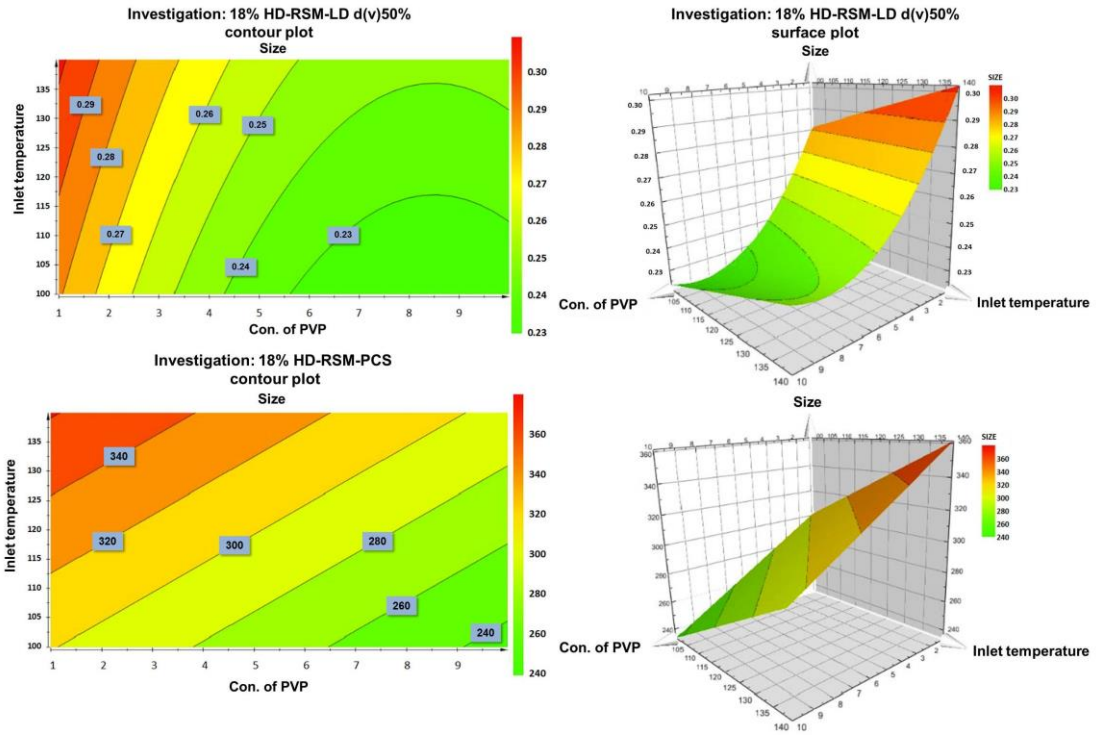

Figure 5-4: The contour plots (left) and surface plots (right) given by the RSM model of MODDE 9 software through the analysis of LD d(v)50% (μm, upper) and PCS (nm, lower) size, sizes are plotted on y-axis.

Figure 5-4 displays the contour plots and surface plots of LD d(v)50% and PCS, respectively. The contour plot obtained from the results of LD d(v)50% indicated that the LD d(v)50% of SNCs could be controlled lower than 0.23 μm when the inlet temperature and the PVP K25 concentration were adjusted within the area under the curve marked 0.23. Similarly, from the contour and surface plots of PCS result, SNCs with 240 nm diameter could be generated with an inlet temperature of 104 ^{o}C and 10% of PVP K25 or an inlet temperature of 100 ^{o}C and 9.2% of PVP K25 in the spray drying.

5.3.3 The prediction list

Table 5-4: The prediction list given by the RSM model of MODDE 9 soft ware through the analysis of LD d(v)50% and PCS size. (Con. PVP = Concentration of PVP).

Con. of PVP (%)	**Inlet temperature (°C)**	**Size-LD d(v)50% (µm)**	**Size-PCS (nm)**
5	100	0.234	271
8	100	0.221	248
10	100	0.224	233

As listed in Table 5-4, the MODDE 9 RSM model predicted the response of LD d(v)50% and PCS based on the previous experiments and the responses. In this prediction, the inlet temperature was fixed at 100 ^{o}C and SNCs with different sizes could be obtained when changing the concentration of PVP K25 added to the hesperidin nanosuspension. To verify the predictions, an experiment was conducted in the present study: 5% (w/w) of PVP K25 was added into the 18% hesperidin nanosuspension, after a complete mixing the nanosuspension was spray dried with an inlet temperature of 100 ^{o}C. Light microscopy, LD and PCS were performed to evaluate the SNCs after the re-dispersion in water.

5.3.4 Characterization of the SNCs

5.3.4.1 Particle size of re-dispersed spray dried product

Figure 5-5 displays the light microscopy images of original hesperidin nanosuspension before spray drying and the obtained re-dispersed SNCs. No agglomeration was observed in the re-dispersed SNCs. Because of the dilution effect during the re-dispersion in water, fewer particles were observed in picture B, compared with picture A.

The key of a successful drug nanoparticle re-dispersion is compensating the extra free energy of exposed surfaces (Choi, Yoo et al. 2005). Ionic surfactants, nonionic surfactants and polymers have been applied commonly in nanocrystals, either as the stabilizers in nanosuspensions or as the protectants in the subsequent transformation

into solid products (Kumar, Gokhale et al. 2014; Ahuja, Jena et al. 2015). In this study, poloxamer 188 was used as the stabilizer in producing hesperidin nanosuspension. As a nonionic hydrophilic surfactant, poloxamer 188 can attach on the surface of nanocrystals generating a strong steric stabilizing effect. It was demonstrated in this study that only 1% (w/w) of poloxamer 188 in the system could prevent the agglomeration of hesperidin nanocrystals.

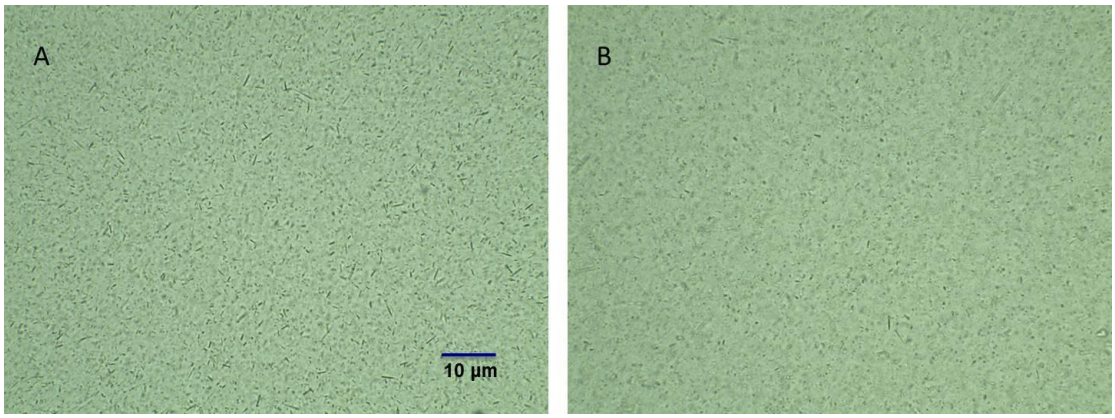

Figure 5-5: Light microscopies of hesperidin nanocrystals before (A) and after (B) spray drying (magnification 400 ×; scale = 10 µm).

Polyvinylpyrrolidone (PVP) K25, one of the highly polar polymers, can also adsorb onto the surface of drug particles and effectively prevent particles aggregation (Niwa and Danjo 2013). However, when the concentration of PVP K25 was relatively low, it was insufficient to form a film with good steric effect against the agglomeration during spray drying. In contrast, when more PVP K25 was added, a protectant film could be formed and the spatial-hindrance effect could inhibit the formation of large particles/aggregates(Xia, Chen et al. 2008). In the re-dispersed SNCs, the PVP K25 supports the stabilizing effect of the poloxamer 188 on the nanocrystals.

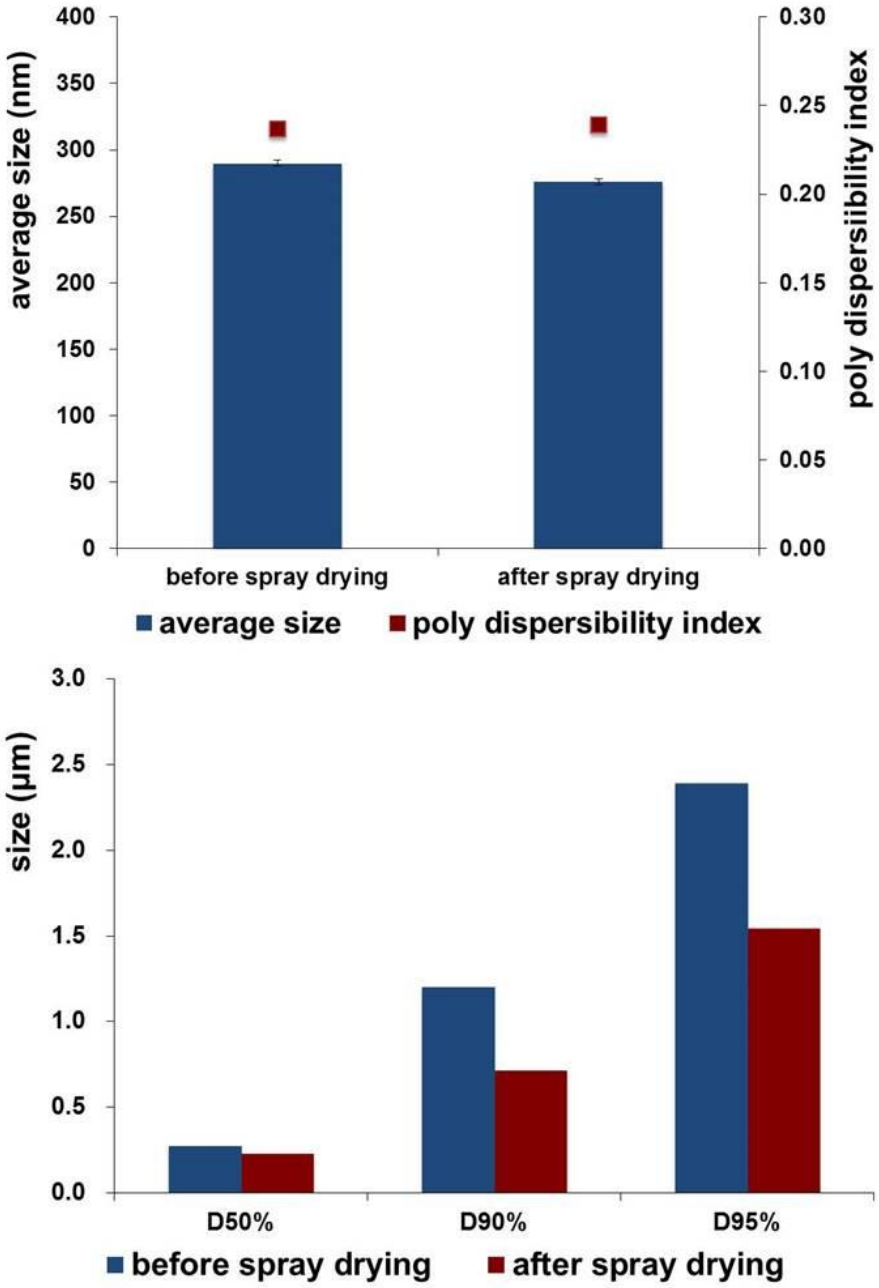

Figure 5-6: PCS (with standard deviation, number of parallel samples: n = 3) (upper) and LD (lower) measured particle sizes before and after spray drying (PI = polydispersity index).

Low inlet temperature was found to be the most important parameter in generating SNCs with improved re-dispersibility. It may be due to that high inlet temperature allows the turbulent motion of nanoparticles, in which case the adherence of protectant molecules onto the nanoparticles could be hindered. However, a definite boundary of protectant could be generated at lower inlet temperature with less nanoparticles

turbulent motion (Vehring, Foss et al. 2007; Paudel, Loyson et al. 2013; Zhang, Guan et al. 2014).

In Figure 5-6 (upper), the PCS graph shows that the size of hesperidin nanoparticles was 290 ± 2.16 nm before and 276 ± 1.98 nm after spray drying, i.e. practically no change. The "slight tendency" in reduction might be explainable by additional steric stabilization effect of the PVP K25 present. Also the PI did not change significantly. Similarly, the LD data show that the re-dispersed nanoparticles after spray drying possessed lower d(v)50%, d(v)(90%) and d(v)(95%) values compared with the original nanoparticles before spray drying. Especially the decrease in the diameters d(v)(90%) and d(v)(95%) indicates the removal of aggregated crystals, explainable by the effect of PVP K25, which is not present in the original dispersion before being processed in spray drying.

5.3.4.2 Crystalline form

DSC and XRD were used to analyze the structural properties of hesperidin SNCs and compare them with the raw material.

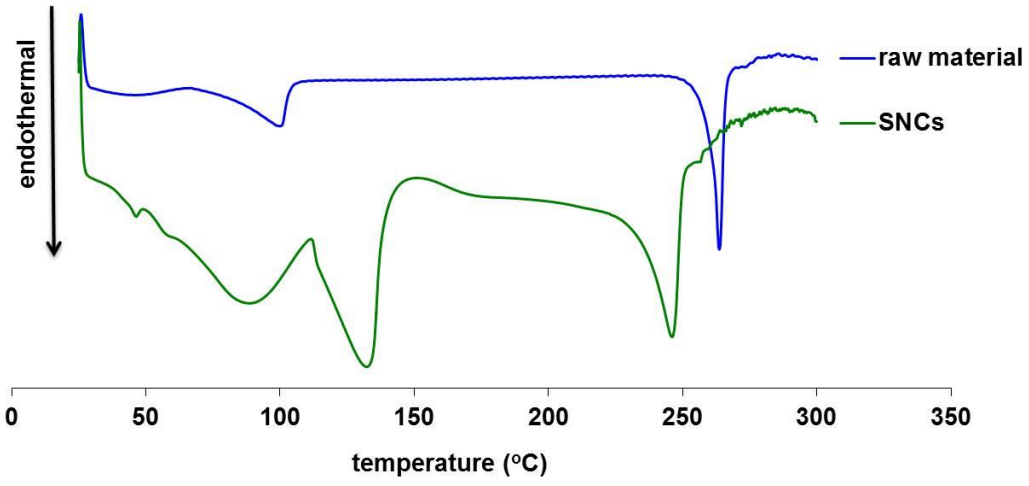

Figure 5-7: DSC thermograms of hesperidin raw material and hesperidin SNCs.

Figure 5-7 shows the DSC results. Hesperidin raw material displayed a melting peak around 265 °C confirming the crystalline structure. A slightly left shift of the melting

peak and the moving down of base line were observed in the SNCs. This could be attributed to the generation of hesperidin solid dispersion in PVP K25. An endothermic peak at 135 ^{o}C was detected due to the melting of PVP K25. The peaks observed around 100 ^{o}C in raw material and the SNCs were because of the evaporation of water retained in the samples.

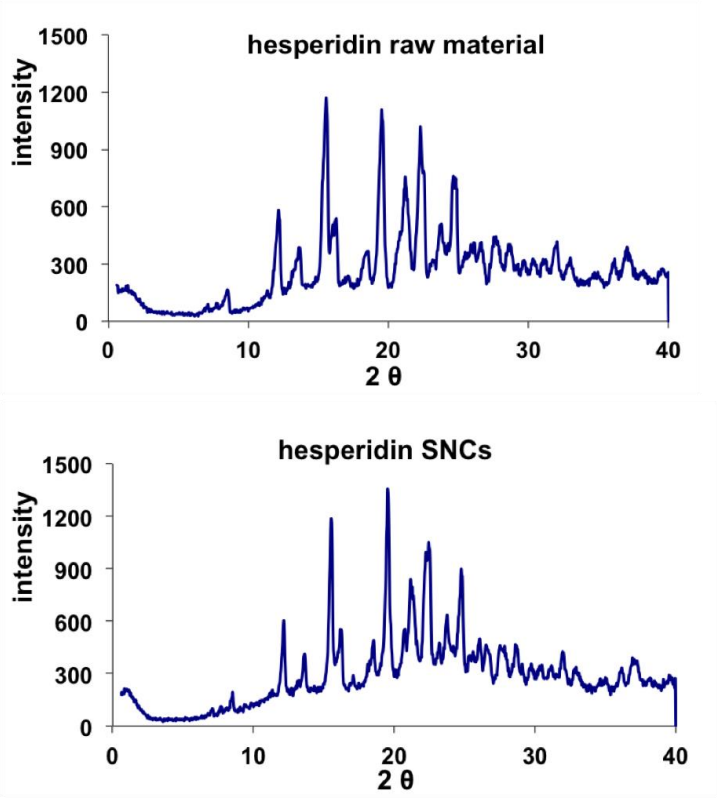

Figure 5-8: X-ray diffractogram patterns of hesperidin raw material and hesperidin SNCs.

XRD results are shown in Figure 5-8. Sharp peaks were observed in hesperidin raw material and the SNCs, which implied that most of the SNCs after spray drying maintained in the crystalline form, based on the detection limit of 5% in XRD analysis being at least 95% crystalline.

5.3.4.3 Kinetic saturation solubility

A 48 h kinetic solubility study was carried out to check the differences in solubility among hesperidin raw material, hesperidin nanosuspension and hesperidin SNCs (Figure 5-9). Due to the crystalline characteristics and µm-crystal size, hesperidin raw

material possessed the lowest saturation solubility. A continuous increase of saturation solubility was observed in all the media and the saturation solubility in water after 48 h reached to 18.03 ± 1.64 μg/ml. The solubility of the nanosuspension was higher, being most pronounced in water and pH 6.8 PBS (roughly about double the concentration of raw material). This could be explained by the Kelvin equation (increased dissolution pressure) (Simonell.Ap, Mehta et al. 1970). A concentration of 34.62 ± 1.38 μg/ml was measured in water after 4 h, which stayed then practically unchanged.

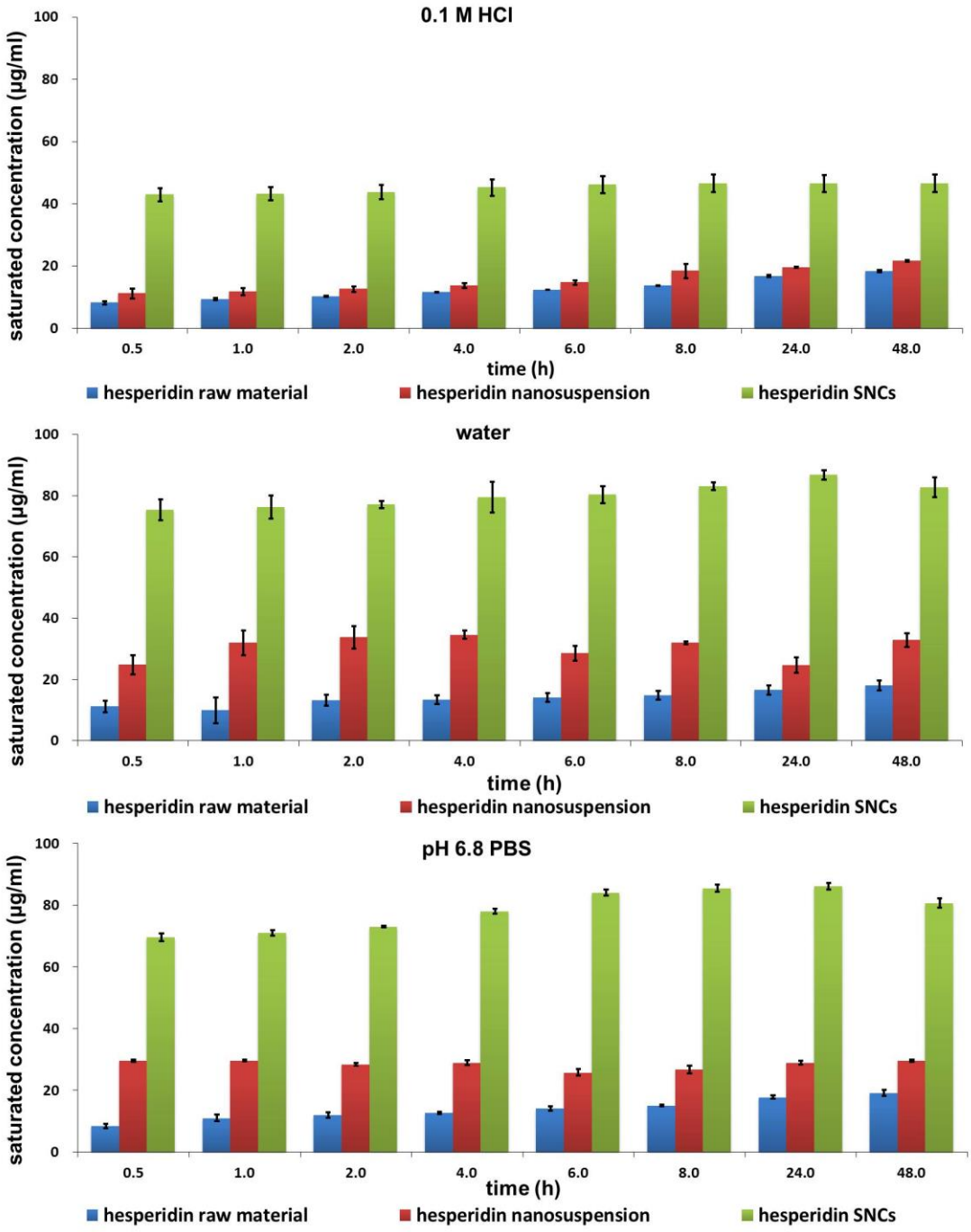

Figure 5-9: Means (bars) and standard deviations (line segments) of saturation solubilities of hesperidin raw material, hesperidin nanosuspension and hesperidin SNCs in different media as a function of time (number of parallel samples: n = 3).

As expected, the hesperidin SNCs showed the highest saturation solubility in all the media. In 0.1 M HCl, the saturation solubility reached to 46.60 ± 2.79 µg/ml after 8 h, in water 86.81 ± 1.51 µg/ml after 24 h, and in pH 6.8 PBS 86.18 ± 1.08 µg/ml after 24 h. The significant improvement of saturation solubility of the SNCs was due not only to the reduction of particle size to a nano range but as well by the generation of solid

dispersion of hesperidin in PVP K25 during the spray drying process. Because the same amount of PVP was added when measuring the solubility of raw material and nanosuspension, it could not be concluded that PVP can solubilize hesperidin directly. But it worked during the process of spray drying. The extremely fine nanocrystals dissolved partially in the suspension and dispersed in amorphous/solid solution state in PVP matrix when the system was dried, therefore the saturation solubility increased. This shows that both the nanonization technology and the spray drying process with a suitable polymer led to the improvement of solubility.

5.3.4.4 In-vitro release study

Figure 5-10 shows the *in-vitro* drug release profiles of hesperidin raw material, hesperidin nanosuspension and the SNCs. Due to the drug content in the marketed tablets, the amount of 50 mg hesperidin was placed per vessel. Owing to the low saturation solubility and µm-crystal size, hesperidin raw material possessed the slowest dissolution rate in all the three media: 10.6 ± 0.7%, 12.3 ± 0.4% and 10.8 ± 0.1% of drug were released after 3 h in 0.1 M HCl, water and pH 6.8 PBS, respectively. Due to the reduction of particle size, hesperidin nanosuspension showed an improved saturation solubility, thereby slightly improved dissolution rate compared to the raw material was observed. 16.1 ± 0.8%, 17.6 ± 1.3% and 13.7 ± 0.4% of hesperidin were released after 3 h in 0.1 M HCl, water and pH 6.8 PBS, respectively. This result can be explained by the Noyes-Whitney equation, proportionality of saturation solubility (Cs) and dissolution rate (dc/dt) leads to faster dissolution of nanosuspensions (Keck and Müller 2006).

It has been known that the amorphous state and wettability both contribute to the fast dissolution rate (Mehanna, Motawaa et al. 2011). The addition of PVP K25 improves drug wettability (Al-Obaidi, Ke et al. 2011). Furthermore, the spray drying process with PVP K25 can solubilize hesperidin. Therefore, the SNCs obtained showed the fastest drug release: 38.9 ± 0.3%, 40.0 ± 1.0% and 43.2 ± 1.7% of hesperidin were measured after 3 h in 0.1 M HCl, water and pH 6.8 PBS, respectively.

The profile of all dissolution curves is biphasic, previously observed for nanosuspension (Mauludin 2008; Mauludin and Müller 2013). After an initial burst release within the first 5 minutes, the profiles level off. This can be explained by the polydispersity of the particle size distribution. The very small nanocrystals (<< 100 nm) show the fastest dissolution (and have the highest saturation solubility, Cs), the remaining crystals dissolve more slowly, and the Cs is also distinctly lower. A very small amount of nanocrystals is present in most raw powders, this explains also the fast release which can occur in mm-sized crystal populations.

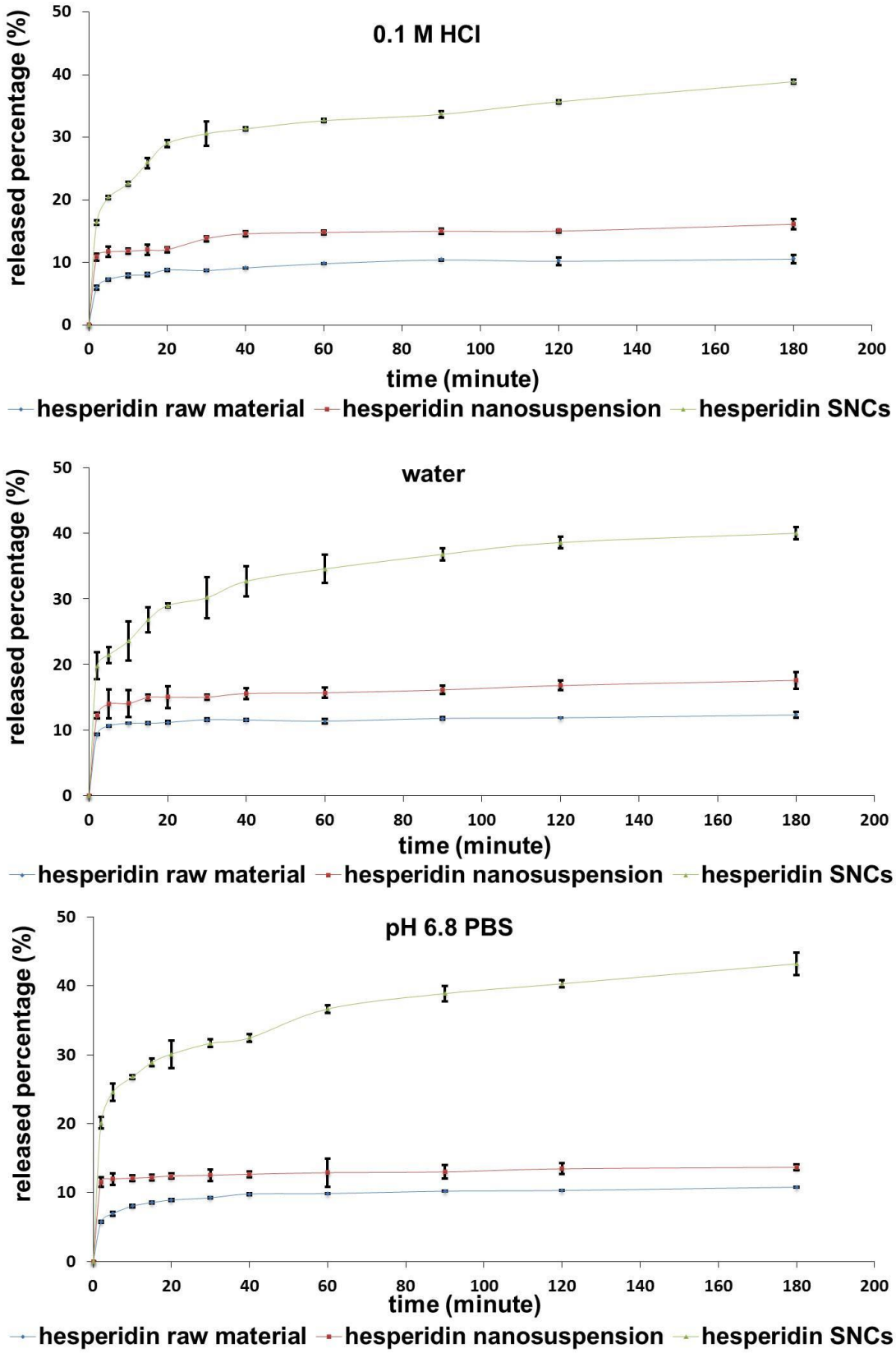

Figure 5-10: Dissolution profiles with standard deviation of hesperidin raw material, hesperidin nanosuspension and hesperidin SNCs in different media as a function of time (number of parallel samples: n = 3).

5.4 Conclusion

A systematic investigation based on DoE principle was conducted to determine the critical factors for the solidification of hesperidin nanocrystals by spray drying. Well re-dispersible nanocrystals could be obtained by using low inlet temperatures (e.g. 100 °C) and medium to high concentrations of PVP K25 (5.5%-10.0%) as protectant. DoE is thus a very helpful tool to replace trial & error concept for solidification of liquid nanosuspensions, prior to conversion to final solid dosage forms.

Using PVP K25 as the protectant during spray drying not only maintained the nanocrystal size (protective matrix), but as well improved the dissolution rate of the hesperidin nanocrystals (steric stabilization to avoid aggregation, solubilization capacity during spray drying). Such effects should be priori considered when selecting protectants for spray drying, and optionally stabilizing the original nanosuspension directly with a polymer suitable as protectant.

5.5 References

Ahuja, B. K., S. K. Jena, et al. (2015). "Formulation, optimization and in vitro-in vivo evaluation of febuxostat nanosuspension." Int J Pharm 478(2): 540-552.

Al-Obaidi, H., P. Ke, et al. (2011). "Characterization and stability of ternary solid dispersions with PVP and PHPMA." Int J Pharm 419(1-2): 20-27.

Bergan, J. J., G. W. Schmid-Schonbein, et al. (2001). "Therapeutic approach to chronic venous insufficiency and its complications: Place of Daflon® 500 mg." Angiology 52: S43-S47.

Bose, S., D. Schenck, et al. (2012). "Application of spray granulation for conversion of a nanosuspension into a dry powder form." Eur J Pharm Sci 47(1): 35-43.

Cal, K. and K. Sollohub (2010). "Spray drying technique. I: Hardware and process parameters." J Pharm Sci 99(2): 575-586.

Chaubal, M. V. and C. Popescu (2008). "Conversion of nanosuspensions into dry

powders by spray drying: a case study." Pharm Res 25(10): 2302-2308.

Choi, J. Y., J. Y. Yoo, et al. (2005). "Role of polymeric stabilizers for drug nanocrystal dispersions." Curr Appl Phys 5(5): 472-474.

Engers, D., J. Teng, et al. (2010). "A solid-state approach to enable early development compounds: selection and animal bioavailability studies of an itraconazole amorphous solid dispersion." J Pharm Sci 99(9): 3901-3922.

Junghanns, J. U. A. H. and R. H. Müller (2008). "Nanocrystal technology, drug delivery and clinical applications." Int J Nanomedicine 3(3): 295-309.

Junyaprasert, V. B. and B. Morakul (2015). "Nanocrystals for enhancement of oral bioavailability of poorly water-soluble drugs." Asian J Pharm Sci 10(1): 13-23.

Keck, C. M. and R. H. Müller (2006). "Drug nanocrystals of poorly soluble drugs produced by high pressure homogenisation." Eur J Pharm Biopharm 62(1): 3-16.

Kipp, J. E. (2004). "The role of solid nanoparticle technology in the parenteral delivery of poorly water-soluble drugs." Int J Pharm 284(1-2): 109-122.

Kumar, S., R. Gokhale, et al. (2014). "Sugars as bulking agents to prevent nano-crystal aggregation during spray or freeze-drying." Int J Pharm 471(1-2): 303-311.

Kumar, S., X. Xu, et al. (2014). "Formulation parameters of crystalline nanosuspensions on spray drying processing: a DoE approach." Int J Pharm 464(1-2): 34-45.

Mauludin, R. (2008). “Nanosuspensions of poorly soluble drugs for oral administration.” Doctoral thesis, Freie Universität Berlin.

Mauludin, R. and R. H. Müller (2013). "Physicochemical properties of hesperidin nanocrystal." Int J Pharm Pharm Sci 5(3): 954-960.

Mehanna, M. M., A. M. Motawaa, et al. (2011). "Tadalafil inclusion in microporous silica as effective dissolution enhancer: optimization of loading procedure and molecular state characterization." J Pharm Sci 100(5): 1805-1818.

Mou, D. S., H. B. Chen, et al. (2011). "Potent dried drug nanosuspensions for oral

bioavailability enhancement of poorly soluble drugs with pH-dependent solubility." Int J Pharm 413(1-2): 237-244.

Nekkanti, V., R. Pillai, et al. (2009). "Development and characterization of solid oral dosage form incorporating candesartan nanoparticles." Pharm Dev Technol 14(3): 290-298.

Niwa, T. and K. Danjo (2013). "Design of self-dispersible dry nanosuspension through wet milling and spray freeze-drying for poorly water-soluble drugs." Eur J Pharm Sci 50(3-4): 272-281.

Noyes, A. and W. Whitney (1897). "The rate of solution of solid substance in their own solutions." J Am Chem Soc 19: 930-934.

Patel, A. D., A. Agrawal, et al. (2014). "Investigation of the effects of process variables on derived properties of spray dried solid-dispersions using polymer based response surface model and ensemble artificial neural network models." Eur J Pharm Biopharm 86(3): 404-417.

Paudel, A., Y. Loyson, et al. (2013). "An investigation into the effect of spray drying temperature and atomizing conditions on miscibility, physical stability, and performance of naproxen-PVP K 25 solid dispersions." J Pharm Sci 102(4): 1249-1267.

Paudel, A., Z. A. Worku, et al. (2013). "Manufacturing of solid dispersions of poorly water soluble drugs by spray drying: formulation and process considerations." Int J Pharm 453(1): 253-284.

Petersen, R. (2008). “Nanocrystals for use in topical cosmetic formulations and method of production thereof.” Patent No.: WO2008058755.

Pilcer, G., F. Vanderbist, et al. (2009). "Preparation and characterization of spray-dried tobramycin powders containing nanoparticles for pulmonary delivery." Int J Pharm 365(1-2): 162-169.

Ramelet, A. A. (2001). "Clinical benefits of daflon 500 mg in the most severe stages of chronic venous insufficiency." Angiology 52: S49-S56.

Scholz, P. and C. M. Keck (2014). "Flavonoid nanocrystals produced by ARTcrystal-technology." Int J Pharm 482(1-2):27-37.

Simonell.Ap, S. C. Mehta, et al. (1970). "Inhibition of Sulfathiazole Crystal Growth by Polyvinylpyrrolidone." J Pharm Sci 59, 633-638.

Sun, W., R. Ni, et al. (2014). "Spray drying of a poorly water-soluble drug nanosuspension for tablet preparation: formulation and process optimization with bioavailability evaluation." Drug Dev Ind Pharm.

Van Eerdenbrugh, B., L. Froyen, et al. (2008). "Drying of crystalline drug nanosuspensions-the importance of surface hydrophobicity on dissolution behavior upon redispersion." Eur J Pharm Sci 35(1-2): 127-135.

Vehring, R., W. R. Foss, et al. (2007). "Particle formation in spray drying." J Aerosol Sci 38(7): 728-746.

Xia, Q., X. Chen, et al. (2008). "Synthesis and characterizations of polycrystalline walnut-like CdS nanoparticle by solvothermal method with PVP as stabilizer." Mater Chem Phys 111(1): 98-105.

Yue, P., C. Wang, et al. (2015). "The importance of solidification stress on the redispersibility of solid nanocrystals loaded with harmine." Int J Pharm 480(1-2): 107-115.

Yuminoki, K., F. Seko, et al. (2014). "Preparation and evaluation of high dispersion stable nanocrystal formulation of poorly water-soluble compounds by using povacoat." J Pharm Sci 103(11): 3772-3781.

Zhang, X., J. Guan, et al. (2014). "Preparation and solidification of redispersible nanosuspensions." J Pharm Sci 103(7): 2166-2176.

6 Summary

1. CapsMorph® technology for oral drug delivery

Hesperidin CapsMorph® was produced by loading drug in mesoporous silica material, AEROPERL® 300 Pharma, through wetness impregnation method. First hesperidin was dissolved in DMSO or a mixture of DMSO and Tween 80, then the solution was added to AEROPERL® 300 Pharma. Hesperidin was encapsulated in mesopores in amorphous state after the elimination of DMSO due to the spatial-constraint effect of tiny mesopores and the H-bonds generated between drug and carrier. It was proven that the addition of Tween 80 decreased the kinetic saturation solubility of hesperidin in CapsMorph® compared with the formulation without Tween 80. Compared to the raw material and nanocrystals, hesperidin CapsMorph® showed significantly improved kinetic saturation solubility and increased dissolution rate.

2. Controlled release of poorly water soluble drug by different loadings in AEROPERL® 300 Pharma

The wetness impregnation method was applied to monitor the loading capacity of AEROPERL® 300 Pharma in terms of hesperidin. When more than 57.5% of hesperidin was loaded in AEROPERL® 300 Pharma crystalline characteristics of hesperidin were detected via XRD and DSC, implying the over-load of the system. Hesperidin CapsMorph® with different drug loadings were obtained by applying different times of drug loading processes. It turned out that with the increase of drug loading, the dissolution rate was decreased. Via adjusting the drug loading, the drug *in-vitro* release rate can be controlled. CapsMorph® with 28.6 wt.% of drug loading showed a complete dissolution behavior within a short period. This may be due to that the low drug loading causes a large drug exposed surface area. When the loaded drug in the mesopores was increased, the exposed drug surface area was decreased because of the overlay of drug molecules.

3. Tablet performance of amorphous rutin in AEROPERL® 300 Pharma

Rutin CapsMorph® powder was produced by loading rutin in AEROPERL® 300 Pharma. The kinetic saturation solubility of rutin CapsMorph® powder in water was

measured as 4.93 ± 0.15 mg/ml, approx. 133-fold of rutin raw material. Rutin CapsMorph® tablet and raw material tablet were prepared by adding Explotab® as a disintegrate and compared with rutin market tablet. Rutin CapsMorph® tablet showed lower hardness compared with the rutin market tablet. Due to the large exposed surface area of amorphous drug the rutin CapsMorph® tablet displayed the fastest dissolution rate, almost 95.6 ± 6.9% of drug was released in water within 5 minutes. However, for the rutin market tablet only 42.7 ± 0.8% of drug release was observed in water after 3 hours.

4. Application of DoE on the solidification of nanosuspension via spray drying method

Wet bead milling was performed to produce hesperidin nanosuspension and poloxamer 188 was used as a stabilizer. The solidification of hesperidin nanosuspension through spray drying was investigated systematically by the principle of design of experiment (DoE). PVP K25 was added in nanosuspension as a protectant before spray drying. MODDE 9 was applied to design the experiment. After the screening modeling and the response surface modeling, the inlet temperature of spray drying and the concentration of PVP K25 were considered as the most important factors affecting the re-dispersion of nanocrystals. Well re-dispersed nanocrystals were obtained when 5.5% of PVP K25 was added in hesperidin nanosuspension and the spray drying was performed under 100 ^{o}C of inlet temperature. Spray drying was demonstrated to be an ideal method to realize the solidification of nanosuspension.

7 Zusammenfassung

1 CapsMorph®-Technologie für die orale Wirkstoffapplikation

Hesperidin CapsMorph® wurde mit der Imprägniermethode durch Beladung von mesoporösem Silica, AEROPERL® 300, hergestellt. Zunächst wurde Hesperdin in DMSO oder einer Mischung von DMSO und Tween 80 gelöst, im nächsten Schritt dann diese Hesperidin-Lösung zu AEROPERL® 300 gegeben. Nach Evaporation des DMSO präzipitierte Hesperidin in den Mesoporen und wurde darin im amorphen Zustand verkapselt aufgrund der räumlichen Einschränkung in den kleinen Mesoporen (2-50 nm) und den H-Bindungen zwischen Wirkstoff und Porenoberfläche des Trägers. Es konnte gezeigt werden, daß der Zusatz von Tween 80 die kinetische Sättigungslöslichkeit im Vergleich zur Formulierung ohne Tween 80 erniedrigte. Im Vergleich zum Rohmaterial (Pulver) und Nanokristallen zeigte Hesperidin CapsMorph® eine signifikant erhöhte kinetische Sättigungslöslichkeit und erhöhte Lösungsgeschwindigkeit.

2 Kontrollierte Freisetzung von schwer wasserlöslichen Wirkstoffen aus AEROPERL® 300 Pharma durch Variation des Beladungsgrades

Unter Verwendung der Imprägniermethode wurde die Beladungskapazität von AEROPERL® 300 Pharma für die Beladung mit Hesperidin untersucht. Wenn eine Beladung von mehr als 57,5% mit Hesperidin erfolgte, konnten kristalline Eigenschaften mit Röntgenstrukturanalyse (X-ray) und DSC detektiert werden, was die Überladung des Systems anzeigte. Hesperidin CapsMorph® mit unterschiedlichen Beladungen wurde kontrolliert erzeugt durch die Anwendung unterschiedlicher Beladungsprozeduren. Es zeigte sich, daß mit ansteigender Beladung die Lösungsgeschwindigkeit abnahm. Dadurch kann durch Variation des Beladungsgrades die in-vitro Freisetzungsgeschwindigkeit von Arzneistoffen kontrolliert werden. CapsMorph® mit 28,6% Beladung zeigte eine komplette Freisetzung innerhalb sehr kurzer Zeit. Dies kann möglicherweise darauf zurückgeführt werden, dass bei niedriger Beladung eine relative große Wirkstoffoberfläche in den Poren in Kontakt mit dem Lösungsmittel steht (keine geschlossenen Poren). Mit ansteigender Beladung nimmt die Oberfläche in den Poren durch zusätzliche Einlagerung von Wirkstoff ab.

3 Tablettierung von amorphem Rutin in AEROPERL® 300 Pharma

Rutin CapsMorph® Pulver wurde hergestellt durch beladen von AEROPERL® 300 Pharma. Die kinetische Sättigungslöslichkeit von Rutin CapsMorph® Pulver in Wasser betrug 4,93 ± 0,15 mg/ml, rund 133-fach höher als die von Rutinpulver. Rutin CapsMorph® Tabletten, und zum Vergleich Tabletten mit Rutinpulver, wurden durch Zugabe von Explotab® als Zerfallshilfsmittel hergestellt, und anschließend mit einem Rutin Marktprodukt verglichen. Die Rutin CapsMorph® Tablette zeigte eine geringere Härte als die Tablette im Markt. Aufgrund der großen Oberfläche des amorphen Rutin und seiner verbesserten Löseeigenschaften zeigte die Rutin CapsMorph® Tablette die höchste Auflösungsgeschwindigkeit, fast 95,6 ± 6,9% des Wirkstoffes wurde innerhalb von 5 Minuten freigesetzt. Im Gegensatz dazu setzte die Tablette vom Markt nur 42,7 ± 0,8% über einen Zeitraum von 3 Stunden frei.

4 Anwendung von DOE zur Optimierung der Sprühtrocknung von Nanosuspensionen

Nanosuspensionen von Hesperidin wurden mit der Rührwerkskugelmühle hergestellt, wobei Poloxamer 188 als Stabilisator benutzt wurde. Sprühtrocknung wurde eingesetzt zur Überführung der wässrigen Nanosuspension in ein Pulver. Die Parameter der Sprühtrocknung wurden mittels “design of experiment” (DOE) optimiert. PVP K25 wurde den Nanosupensionen als “Protectant” zur Minimierung der Kristallaggregation zugesetzt. MODDE 9 wurde zur Plaung der Experimemte verwendet. Nach erfolgtem “screening modeling” und “response surface modeling” wurden die Einlasstemperatur beim Sprühtrocknen und die Konzentration an PVP K25 als die bestimmenden Parameter für die anschließende Redispergierbarkeit der Nanokristalle identifiziert. Gut redispergierbare Nanokristalle wurden erhalten nach Zugabe von 5,5% an PVP K25 zur Nanosuspension und anschließendem Sprühtrocknen mit 100 °C Einlasstemperatur. Sprühtrocknung ist eine ideale Methode zur Trocknung.

Statistics

The section declares the statistics applied in this thesis.

In this study, firstly, hesperidin and rutin CapsMorph® were prepared, and the characteristics were evaluated by using light microscopy, scanning electron microscopy, X-ray diffraction, differential scanning calorimetry, and the saturation solubilities and *in-vitro* release profiles were obtained. Secondly, hesperidin nanosuspension was produced and spray dried to obtain the well re-dispersable nanocrystals through a DoE design. Similarly, the characteristics of the solid nanocrystals were evaluated and compared with the original nanosuspension or raw material.

After the production of hesperidin and rutin CapsMorph® samples, light microscopy, scanning electron microscopy, X-ray diffraction and differential scanning calorimetry were performed as single measurement respectively for each sample to confirm the amorphous state and monitor the drug loading process, and for each measurement only one result was shown in the thesis. This is due to the nature of the analysis, and no quantitative evaluation was performed (e.g. in X-ray), which might require statistical comparison. In addition, DSC and X-ray of samples were performed multiple times during storage in order to confirm the amorphous character of the formulations.

Saturation solubilities and *in-vitro* release profiles were determined in triplicate to calculate the means and standard deviations. In general the standard deviations were very low, sometimes lower than the symbol size in the figures (e.g. Fig. 2-7 (page 49), Fig. 3-8 (page 76) etc.), nevertheless they were plotted in all applicable graphs.

Hardness and disintegrating tests of the tablets were performed in triplicate to calculate the means and standard deviations as well.

In this study, the main work was to study the saturation solubilities and *in vitro* release of the developed formulations and to compare them with the traditional formulations. If the saturation solubilities (Cs) of the amorphous formulations were different to the traditional formulations, inter-formulation statistical analysis was not necessary due to

the obviousness of the data (e.g. Cs about 100 x higher than the raw material, e.g. fig. 4-6 (page 96)).

In addition, a large-scale production method (wetness bead milling) was employed to produce hesperidin nanosuspension. Except the light microscopy, scanning electron microscopy, x-ray diffraction, differential scanning calorimetry were used to measure the characteristics of samples, and the saturation solubilities and *in-vitro* release profiles were obtained similarly as above, particle size measurements by photon correlation spectroscopy were performed ten times in triplicate per sample to calculate the means and standard deviations. However, the measurements by laser diffractometry were performed using the setting of 5 measurement runs to obtain a final mean value of single sample, therefore the values shown in this thesis are all means.

In this thesis, the experiment process was detailed by adding the number of independent experiments and parallel samples, and the standard deviation of the values that repeated in triplicate. Of course, the figures include the standard deviations where applicable.

It is remarked that this statement would be statistically more convincing if there had been more parallel samples, which leaves space for future research.

Abbreviations

BCS	Biopharmaceutics Classification System
DMSO	dimethyl sulfoxide
DoE	design of experiment
DSC	differential scanning calorimetry
FDA	US Food and Drug Administration
HCl	hydrochloric acid
HD-CM-28	28.6 wt.% hesperidin CapsMorph®
HD-CM-54	54.5 wt.% hesperidin CapsMorph®
HD-CM-60	60.0 wt.% hesperidin CapsMorph®
HPLC	high performance liquid chromatography
IUPAC	International Union of Pure and Applied Chemistry
LD	laser diffractometry
NT	without Tween 80
PBS	phosphate buffer saline
PCS	photon correlation spectroscopy
PI	polydispersity index
PVP	polyvinylpyrrolidone
RSM	response surface model
SC-CO_2	super-critical CO_2
SEM	scanning electron microscopy

SNCs	solid nanocrystals
UV	ultraviolet
WT	with Tween 80
XRD	X-ray diffraction

Acknowledgements

Prof. Dr. Rainer H. Müller kindly provided his guidance, supervision, suggestion as well as encouragement during my research study and the compilation of this thesis as my doctoral study supervisor. I have learned so much from him about the attitude towards the science research, the methodology for experiment and the mindset to pursue the most innovative breakthroughs. That's why firstly I must express my sincere gratitude to Prof. Dr. Rainer H. Müller.

Secondly I appreciate the guidance of Prof. Dr. Cornelia M. Keck. She also instructed my research path at the beginning of my doctoral study. Her expertise triggered many ideas, which helped me solve the problems in the lab work and paper writing.

I would like to thank China Scholarship Council for providing three-year doctoral scholarship to support my study in Freie Universität Berlin.

I would like to thank PharmaSol GmbH (Berlin, Germany) for R&D support.

Many thanks to Ms. Gabriela Karsubke, Ms. Corinna Schmidt, Ms. Inge Volz, Dr. Lothar Schwabe, Dr. Wolfgang Mehnert and Mr. Alfred Protz for their help and advice in practical issue.

I would like to thank Mr. Frank Odei Addo, Dr. Zhai Xuezhen and Ms. Sung Min Pyo. They were my lab mates and helped me a lot in daily lab affairs. We supported each other.

Special thanks to Dr. Hu Xiaoying, Dr. Liu Tao, Jin Nan and Li Xiangyu for their generous support in our lab during my thesis writing process.

I would like to thank Ms. Daisy Fung for her careful proofreading of part of this thesis.

Last but not least, I would like to reserve my particular gratitude to my husband, my parents and all my family members for their love and support.

List of Publications

Peer-reviewed papers

1. Wei, Q., Müller, R. H., Keck, C. M., Solidification of hesperidin nanosuspension by spray drying optimized by Design of Experiment (DoE), Drug Development and Industrial Pharmacy, in press.
2. Wei, Q., Keck, C. M., Müller, R. H., Preparation and tableting of long-term stable amorphous rutin using porous silica. European Journal of Pharmaceutics and Biopharmaceutics, 2017, 113(3-4): 97–107.
3. Wei, Q., Keck, C. M., Müller, R. H., Oral hesperidin - amorphization & improved dissolution properties by controlled loading onto porous silica. International Journal of Pharmaceutics, 2017, 518(1–2): 253–263.
4. Wei, Q., Keck, C. M., Müller, R. H., CapsMorph® technology for oral delivery--theory, preparation and characterization. International Journal of Pharmaceutics. 2015, 482(1-2): 11-20.

Proceedings

1. Wei, Q., Keck, C. M., Müller, R. H., CapsMorph - amorphous formulation technology for oral delivery of poorly soluble drugs, #2-7, p. 34, CRS Local Chapter Germany, Basel, 12-13 February 2015
2. Wei, Q., Müller, Keck, C. M., Comparison of CapsMorph and nanocrystals of poorly soluble drugs, #644, Int. Symp. Control. Rel. Bioact. Mater. 41, Chicago/Illinois, 13-16 July 2014
3. Müller, R. H., Keck, C. M., Wei, Q., Amorphous drugs in porous materials - stability, solubility & tablet performance, #642, Int. Symp. Control. Rel. Bioact. Mater. 41, Chicago/Illinois, 13-16 July 2014
4. Müller, R. H., Wei, Q., Keck, C. M., CapsMorph: >4 Years long-term stability of industrially feasible amorphous drug formulations, #833, Int. Symp. Control. Rel. Bioact. Mater. 40, Honolulu/Hawaii, 21-24 July 2013

Abstracts

1. Wei, Q., Keck, C. M., Müller, R. H. CapsMorph - amorphous oral delivery technology in porous particles. W4224, AAPS Annual Meeting, Orlando, 25-29

October 2015

2. Wei, Q., Staufenbiel, S., Müller, R. H., Keck, C. M., CapsMorph: controlled release of poorly water-soluble drug by using porous silica material, W5172, AAPS Annual Meeting, San Diego, 2-6 November 2014
3. Wei, Q., Chen, R., Müller, R. H., Keck, C. M., Amorphous CapsMorph with high drug loading capacity for oral formulation, p. 31, 11th European Workshop on Particulate Systems (EWPS), Utrecht, 13-14 March, 2014
4. Wei, Q., Müller, R. H., Romero, G. B., Keck, C. M., Solidification of nanocrystals formulation by spray drying, W5071, AAPS Annual Meeting, San Antonio, 10-14 November 2013
5. Müller, R. H., Wei, Q., Keck, C. M., Stability of industrially feasible amorphous drug formulations generated in porous silica, W5313, AAPS Annual Meeting, San Antonio, 10-14 November 2013
6. Müller, R. H., Wei, Q., Keck, C. M., CapsMorph: >4 Years long-term stability of industrially feasible amorphous drug formulations, p. 50, 7th Polish-German Symposium on Pharmaceutical Sciences: Interdisciplinary research for Pharmacy, Gdansk, 24-25 May 2013
7. Wei, Q., Keck, C. M., Müller, R. H., Amorphous oral nutriceuticals based on aeropearl, W5060, AAPS Annual Meeting, Chicago, 14-18 October 2012
8. Mishra, M., Wei, Q., Shegokar, R., Gohla, S., Müller, R. H., Improvement of human skin penetration of hesperitin from nanocrystal formulation, R6144, AAPS Annual Meeting, Chicago, 14-18 October 2012
9. Wei, Q., Keck, C. M., Müller, R. H., CapsMorph™ – physically stable & industrially feasible amorphous oral delivery technology, PP83, 9th Central European Symposium on Pharmaceutical Technology (CESPT), Dubrovnik, 20-22 September 2012
10. Wei, Q., Keck, C. M., Müller, R. H., CapsMorph-amorphous formulation technology for oral delivery of poorly soluble drugs, P2-7, CRS Germany Local Chapter Meeting, Würzburg, 29-30 March 2012